

Finite Elements and Virtual Elements on Classical Meshes

Franco Brezzi¹ · Luisa Donatella Marini^{2,1}

Received: 26 May 2020 / Accepted: 12 October 2020

Abstract Among Numerical Methods for PDEs, the Virtual Element Methods were introduced recently in order to allow the use of decompositions of the computational domain in polytopes (polygons or polyhedra) of very general shape. The present paper investigates the possible interest in their use (together or in alternative to Finite Element Methods) also for *traditional* decompositions (in triangles, tetrahedra, quadrilateral or hexahedra). In particular their use looks promising in problems related to high-order PDEs (requiring C^p finite dimensional spaces with $p \geq 1$), as well as problems where incompressibility conditions are needed (e.g. Stokes), or problems (like mixed formulation of elasticity problems) where several useful features (symmetry of the stress tensor, possibility to hybridize, \inf -sup stability condition, etc.) are requested at the same time.

Keywords Virtual elements · Finite elements · Polygonal decompositions

Mathematics Subject Classification (2010) 65N30

1 Introduction

Virtual Element Methods (VEM) are a recent technology in Scientific Computing, designed to use decompositions of the computational domain into polygons or polyhedra. As it is well known, the decompositions commonly used by the Finite Element community and in the related commercial codes, so far, have been almost exclusively concentrated on triangles, tetrahedra, quadrilaterals, hexahedra and little more. VEM, instead, are conceived for allowing also complicated geometries, typically polytopes with many faces/edges and complicated

Dedicated to Enrique Zuazua with great esteem and affection.

✉ Luisa Donatella Marini
marini@imati.cnr.it

Franco Brezzi
brezzi@imati.cnr.it

¹ IMATI del CNR, Via Ferrata 1, 27100 Pavia, Italy

² Dipartimento di Matematica, Università di Pavia, Pavia, Italy

shapes. The purpose of the present paper is to show that VEM can also prove to be interesting on simple geometries. Escaping the limit of piecewise polynomial shape functions, VEM can indeed allow more performant local spaces, and could, whenever convenient, be used also on simpler elements, like triangles, quads, and their 3d counterpart. Hence, they could as well be included as useful variants in a Finite Element code.

Indeed, we shall see that even on simple geometries Virtual Elements might come out to be extremely useful, both when used in combination with Finite Elements and when used as an innovative powerful alternative. Throughout the paper we will keep comparing VEM and FEM: we would like to point out, from the very beginning, that this should not be taken as a (rather childish) competition between two very useful instruments. In most cases the main purpose of the *comparison with FEM* will be to help the reader towards a better understanding of the new instrument (with its pros and cons) just by comparing with an instrument that is already well known, and concentrating on the differences. One should keep in mind that the main original motivation for VEM is *to deal with decompositions that are geometrically complicated* and not to *replace FEM on simpler cases*. However, the use of VEM on simple geometries might also prove to be convenient on several occasions.

Actually we shall see that the possibility of adding to the polynomial spaces a few *additional non polynomial functions* can alleviate many types of troubles and give rise to very interesting alternatives. These additional functions are *never* computed explicitly, but one can use, in the code, some related quantities (typically, some kinds of projection) that are computable directly out of the degrees of freedom.

As examples of use of VEM on simple geometries that perform easily where FEM pose nontrivial difficulties, in this paper we take: the use of C^p discretizations (for $p \geq 1$), the treatment of the incompressibility condition for Fluids and for Elastic Materials, and the mixed (stress-displacement) formulation of linear elasticity problems *à la* Hellinger Reissner. We will see that the construction of H^s -conforming approximations (for $s \geq 2$), the use of perfectly incompressible approximations, as well as the use of symmetric-and hybridizable stress fields come out more easily in the VEM context than in the traditional FEM approaches.

An outline of the paper is as follows. In the next section, we will present the basic ideas of Virtual Element Methods, taking as a first example the simple Poisson problem. We will show how to deal with the non-polynomial functions appearing in the local spaces, how to construct a consistent *conforming* approximation, and how to stabilize it in order to get a well-posed discrete problem. Next, a sort of Serendipity procedure will be presented for reducing the number of degrees of freedom internal to the elements. We will see that on triangles Serendipity VEM coincide exactly with the usual polynomial approximation, while on quads we have several little variants that might have some interest here and there. Finally, we will present the *nonconforming* VEM-approximation where some differences between FEM and VEM start to pop out already on triangles.

In Section 3, we will consider the VEM approximation of vector spaces like $H(\text{div}; \Omega)$ and $H(\text{rot}; \Omega)$, and in the following Section 4 we will show how the VEM approach can easily help in the construction of C^1 elements (to deal, e.g., with plate problems). We shall also see that, in the VEM context, the construction of C^p discretized spaces for $p \geq 2$ becomes reasonably feasible, whereas (as is well known) with FEM the construction of C^1 spaces poses already several difficulties.

Next, in Section 5 we will deal with the incompressibility problem. The treatment of these problems in the FEM context has been the object of a number of quite interesting papers in the recent years. Here, a general comparison between VEM and FEM becomes nearly unfeasible, since every FEM approach is different and has different features, pros and cons. We took a (questionable) decision: to make the comparison of VEM with some older and well

known method (actually the Crouzeix–Raviart: \mathbb{P}_2 +bubbles velocities and discontinuous \mathbb{P}_1 pressures). This is, in our opinion, justified by our target of *helping in understanding VEM*, and not *fighting for being the best method* (whatever that means...). We provide however a rich list of references to the latest, quite interesting, FEM developments.

Finally, in the last Section 6 we deal with the Hellinger–Reissner mixed formulation of linear elasticity. Here, we face a situation quite similar but even worse than that of the previous section, in the presence of a wealth of recent different FEM approaches trying to satisfy, at the same time, a number of important requests (stability, symmetry of the stress tensor, possible hybridization, etc.). Here too we decided to compare the VEM approach with one of the best known FEM approach (the Arnold–Awanou–Winther element), although the most similar FEM approach would have been the one by Guzman–Neilan in [38], that however would have required a more detailed description.

1.1 Notation

Throughout the paper, if k is an integer ≥ 0 , \mathbb{P}_k will denote the space of polynomials of degree $\leq k$. In \mathbb{R}^d its dimension $\pi_{k,d}$ is given by:

$$\pi_{k,1} = k + 1, \quad \pi_{k,2} = (k + 1)(k + 2)/2, \quad \pi_{k,3} = (k + 1)(k + 2)(k + 3)/6.$$

As usual, $\mathbb{P}_{-1} = \{0\}$. When no confusion can occur, we will use the simpler π_k .

Next, for a domain \mathcal{O} we will denote by $\Pi_k^{0,\mathcal{O}}$ (or simply by Π_k^0 when no confusion can occur) the $L^2(\mathcal{O})$ -orthogonal projection operator onto $\mathbb{P}_k(\mathcal{O})$, defined, as usual, for every $v \in L^2(\mathcal{O})$, by

$$\Pi_k^{0,\mathcal{O}}(v) \in \mathbb{P}_k(\mathcal{O}) \quad \text{and} \quad \int_{\mathcal{O}} (v - \Pi_k^{0,\mathcal{O}}(v)) q_k d\mathcal{O} = 0 \quad \forall q_k \in \mathbb{P}_k(\mathcal{O}).$$

For s integer ≥ 1 we define also

$$\widehat{\mathbb{P}}_s(\mathcal{O}) := \left\{ q_s \in \mathbb{P}_s \text{ such that } \int_{\mathcal{O}} q_s d\mathcal{O} = 0 \right\}.$$

and assuming the origin to be in the barycenter of \mathcal{O} :

$$\mathbb{P}_s^{\text{hom}}(\mathcal{O}) := \{\text{homogeneous polynomials of degree } s\}.$$

Moreover, given a function $\psi \in L^2(\mathcal{O})$ and an integer $s \geq 0$, we recall that the *moments of order $\leq s$ of ψ on \mathcal{O}* are defined as:

$$\int_{\mathcal{O}} \psi q_s d\mathcal{O} \quad \text{for } q_s \in \mathbb{P}_s(\mathcal{O}).$$

Hence, *to assign the moments of ψ up to the order s on \mathcal{O}* will amount to π_s conditions. Typically this will be used when these moments are considered as *degrees of freedom*. Then, we will take in \mathbb{P}_s a basis $\{q_i\}$ such that $\|q_i\|_{L^1} \simeq 1$.

We recall that, in two dimensions, the **curl** operator has two aspects (as **grad** and **div**) given by

$$\text{rot}(v_1, v_2) := \partial_x v_2 - \partial_y v_1, \quad \text{rot}(\varphi) := (\partial_y \varphi, -\partial_x \varphi).$$

Finally, for a vector $\mathbf{v} = (v_1, v_2)$ we indicate by \mathbf{v}^\perp the vector $\mathbf{v}^\perp = (v_2, -v_1)$.

Throughout the paper we will follow the common notation for scalar products, norms, and seminorms. In particular, $(v, w)_{0, \mathcal{O}}$ (sometimes, just $(v, w)_0$) and $\|v\|_{0, \mathcal{O}}$ (sometimes, just $\|v\|_0$) will denote the $L^2(\mathcal{O})$ scalar product and norm, whereas $|v|_{1, \mathcal{O}}$ (sometimes, just $|v|_1$) and $\|v\|_{1, \mathcal{O}}$ (sometimes, just $\|v\|_1$) will denote the H^1 semi-norm and norm.

Finally, we point out that throughout the paper, as common in the VEM literature, we will consider that the same geometrical entity (say, a triangle) might be considered as a polygon (for instance, a quadrilateral or a pentagon, hexagon, etc.) according to the number of points on its boundary that we consider as *vertices* (and, as natural, considering as *edge* the portion of boundary in between two consecutive vertices, in the usual counterclockwise ordering. See Fig. 1. This feature can be extremely helpful for example when doing adaptive mesh refinement (see the leftmost case in Fig. 1).

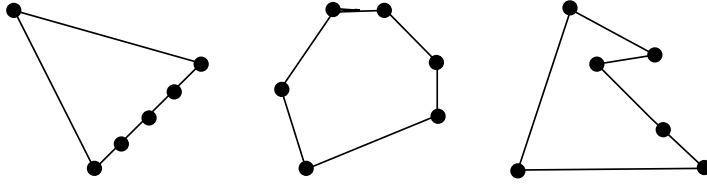


Fig. 1 Each of the three above polygons is considered as a hexagon

2 H^1 Approximations

Let us consider a second order linear elliptic problem, with variational formulation

$$\text{find } u \in V \text{ such that } a(u, v) = \langle f, v \rangle \quad \forall v \in V. \quad (1)$$

To fix ideas one may think of the usual toy problem $-\Delta u = f$ in Ω , $u = 0$ on $\partial\Omega$, with $\Omega \subset \mathbb{R}^2$ a polygonal domain, $f \in L^2(\Omega)$, and $V = H_0^1(\Omega)$, although what follows applies to more general operators. Problem (1) is then

$$\text{find } u \in V = H_0^1(\Omega) \text{ such that } \int_{\Omega} \nabla u \cdot \nabla v \, dx = \int_{\Omega} f v \, dx \quad \forall v \in V.$$

Let \mathcal{T}_h be a decomposition of Ω into polygons \mathcal{P} , and let $V_h \subset V$ be a finite dimensional subspace. We can write the discrete problem as

$$\text{find } u_h \in V_h \text{ such that } a_h(u_h, v_h) = \langle f_h, v_h \rangle \quad \forall v_h \in V_h, \quad (2)$$

and we have to define V_h , $a_h(\cdot, \cdot)$, and f_h in such a way that problem (2) has a unique solution and optimal error estimates hold. In the next subsection we will recall the original approach of [15] and indicate the general path of Virtual Element approximations.

2.1 Original Virtual Element Approximation

We first recall the definition of the discrete spaces from [15]. Let \mathcal{P} be a generic polygon in \mathcal{T}_h . For $k \geq 1$ we define

$$V_k(\mathcal{P}) := \left\{ v \in C^0(\overline{\mathcal{P}}) : v|_e \in \mathbb{P}_k(e) \forall \text{ edge } e \subset \partial\mathcal{P}, \Delta v \in \mathbb{P}_{k-2}(\mathcal{P}) \right\}, \quad (3)$$

with the degrees of freedom given by

$$\begin{aligned} (D_1) &: \text{ the values of } v \text{ at the vertices,} \\ (D_2) &: \text{ for } k \geq 2 \text{ the moments } \int_e v p_{k-2} ds \quad \forall p_{k-2} \in \mathbb{P}_{k-2}(e) \quad \forall \text{ edge } e, \\ (D_3) &: \text{ for } k \geq 2 \text{ the moments } \int_{\mathcal{P}} v p_{k-2} dx \quad \forall p_{k-2} \in \mathbb{P}_{k-2}(\mathcal{P}). \end{aligned} \quad (4)$$

Instead of the moments D_2 one could use the values at $k-1$ distinct points on each edge, more in the spirit of FEM:

$$(D'_2) : \text{ the value of } v \text{ at } k-1 \text{ distinct points on each edge } e.$$

The global space is then defined as

$$V_h := \{ v \in V : v|_{\mathcal{P}} \in V_k(\mathcal{P}) \quad \forall \mathcal{P} \in \mathcal{T}_h \}. \quad (5)$$

It can be shown ([15]) that out of the dofs (4) we can compute on each element \mathcal{P} the operator $\Pi_k^\nabla : V_k(\mathcal{P}) \rightarrow \mathbb{P}_k(\mathcal{P})$ defined by

$$\int_{\mathcal{P}} \nabla \left(\Pi_k^\nabla v - v \right) \cdot \nabla q_k dx = 0 \quad \forall q_k \in \mathbb{P}_k, \quad \int_{\partial\mathcal{P}} \left(\Pi_k^\nabla v - v \right) ds = 0. \quad (6)$$

Then, a discrete bilinear form is constructed, on each element \mathcal{P} , as

$$a_h^\mathcal{P}(v_h, w_h) := a^\mathcal{P} \left(\Pi_k^\nabla v_h, \Pi_k^\nabla w_h \right) + S^\mathcal{P} \left(\left(I - \Pi_k^\nabla \right) v_h, \left(I - \Pi_k^\nabla \right) w_h \right) v_h, \quad w_h \in V_h, \quad (7)$$

where $S^\mathcal{P}$ is any symmetric bilinear form that scales like $a^\mathcal{P}(\cdot, \cdot)$. There are various recipes for $S^\mathcal{P}$, the most commonly used being the so-called *dofi-dofi*:

$$S^\mathcal{P}(v_h, w_h) := \sum_{i=1}^{\#dofs} dofi_i(v_h) dofi_i(w_h). \quad (8)$$

We can also define a right-hand side f_h directly computable from the degrees of freedom (D_1) – (D_3) . Denoting by V_1, \dots, V_n the vertices of \mathcal{P} we set:

$$\langle f_h, v_h \rangle_{\mathcal{P}} = \begin{cases} \text{for } k = 1 & \int_{\mathcal{P}} \Pi_0^0 f \bar{v}_h dx \quad \text{with } \bar{v}_h = \frac{\sum_i v_h(V_i)}{n}, \\ \text{for } k \geq 2 & \int_{\mathcal{P}} \Pi_{k-2}^0 f v_h dx. \end{cases} \quad (9)$$

The global bilinear form and right-hand side are defined, as in FEM, by summing over the elements of \mathcal{T}_h :

$$a_h(v_h, w_h) = \sum_{\mathcal{P} \in \mathcal{T}_h} a_h^\mathcal{P}(v_h, w_h), \quad \langle f_h, v_h \rangle = \sum_{\mathcal{P} \in \mathcal{T}_h} \langle f_h, v_h \rangle_{\mathcal{P}}.$$

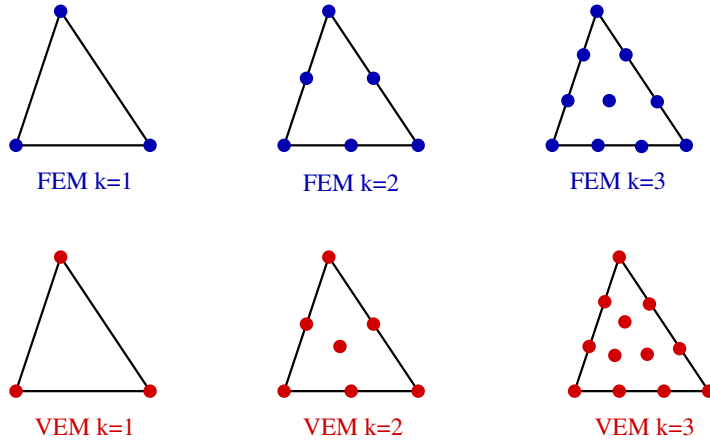


Fig. 2 Triangles: d.o.f.s for FEM and original VEM

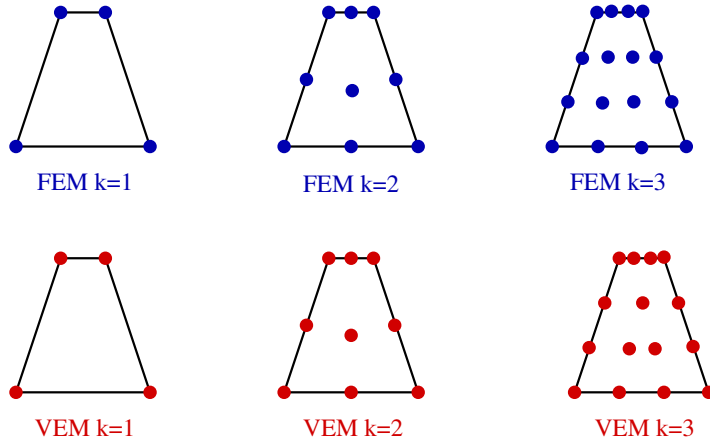


Fig. 3 Quads: d.o.f.s for FEM and original VEM

With these choices (and mild assumptions on the mesh) it has been proved that problem (2) has a unique solution, and optimal estimates hold

$$\|u - u_h\|_V \leq Ch^k |u|_{k+1}.$$

Figures 2 and 3 show a comparison between FEM and VEM on triangles and quads.

From Fig. 2 we see that triangular VEM have more degrees of freedom than FEM for $k \geq 2$. Looking for simplicity at the case $k = 2$ we point out that the additional degree of freedom in the VEM space corresponds to the function β_2 defined by:

$$\beta_2 = 0 \text{ on } \partial\mathcal{P}, \quad \text{and} \quad \Delta\beta_2 = 1 \text{ in } \mathcal{P} \quad (10)$$

that, clearly, is not in \mathbb{P}_2 .

Instead, from Fig. 3 we see that for quads VEM have less degrees of freedom for $k \geq 3$: indeed, the number of internal d.o.f.s for FEM equals the dimension of \mathbb{Q}_{k-2} , i.e. $(k-1)^2$,

while that of VEM is equal to the dimension of \mathbb{P}_{k-2} , given by $k(k-1)/2$. We also underline that, as it can be seen in Figs. 2–3, the internal dofs for VEM do not change with the element shape; what changes when going from a triangle to a quad or to a generic polygon is just the number of edge-dofs, which depends on the number of edges.

2.2 Enhanced and Serendipity Virtual Elements

Following [1] and [17], in order to eliminate as many internal dofs as possible, and, at the same time, to allow the computation of all the moments of order $\leq k$, we first define the local space

$$\tilde{V}_k^S(\mathcal{P}) := \{v \in C^0(\bar{\mathcal{P}}) : v|_e \in \mathbb{P}_k(e) \forall e \subset \partial\mathcal{P}, \Delta v \in \mathbb{P}_k(\mathcal{P})\}, \quad (11)$$

with the degrees of freedom

$$(D_1) - (D_2) \quad \text{plus the moments of order up to } k : \int_{\mathcal{P}} v p_k dx \quad \forall p_k \in \mathbb{P}_k(\mathcal{P}).$$

Clearly the space (11) is bigger than (3), apparently in contradiction with our first aim, but now the L^2 -orthogonal projection onto \mathbb{P}_k is directly available from the internal dofs. Then we begin by defining locally an operator $\Pi_k : H^1(\mathcal{P}) \rightarrow \mathbb{P}_k(\mathcal{P})$ as follows:

$$\Pi_k v \in \mathbb{P}_k(\mathcal{P}) : \int_{\partial\mathcal{P}} (\Pi_k v - v) q_k ds = 0 \quad \forall q_k \in \mathbb{P}_k(\mathcal{P}). \quad (12)$$

Clearly, system (12) has a unique solution unless \mathbb{P}_k contains polynomials that are identically zero on the boundary, i.e., unless \mathbb{P}_k contains bubbles. This happens for $k \geq 3$ on triangles ($b_3 =$ product of the equations of the three edges) and for $k \geq 4$ on “true” quads ($b_4 =$ product of the equations of the four edges). In these cases we need to add internal conditions, namely:

$$\underbrace{\int_{\mathcal{P}} (\Pi_k v - v) q_s dx = 0 \quad \forall q_s \in \mathbb{P}_{k-3}}_{\text{on triangles}} \quad \text{or} \quad \underbrace{\int_{\mathcal{P}} (\Pi_k v - v) q_s dx = 0 \quad \forall q_s \in \mathbb{P}_{k-4}}_{\text{on quads}}, \quad (13)$$

and then solve the system (12)–(13) in the least-squares sense. Once the polynomial $\Pi_k v$ has been computed, we define the new space by “copying” its moments. Namely, setting $N =$ maximum degree of internal moments used to define Π_k :

$$V_k^S(\mathcal{P}) := \left\{ v \in \tilde{V}_k^S(\mathcal{P}) \text{ s.t. } \int_{\mathcal{P}} v p_s dx = \int_{\mathcal{P}} \Pi_k v p_s dx \quad \forall p_s \in \mathbb{P}_s^{hom}, N < s \leq k \right\} \quad (14)$$

Figure 4 shows that on triangles serendipity VEM have the same number of dofs as FEM (and actually the two spaces *coincide*), while Fig. 5 compares the dofs of serendipity VEM and FEM (see [3]). The number is the same, although serendipity FEM are known to suffer from distortion (see [6]), while VEM do not, as shown in [17].

A typical variant of this procedure can be identified in the original *enhancement trick* as designed first in [1]. For a given integer $\delta \geq k - 2$ one considers the space

$$\tilde{V}_\delta^E(\mathcal{P}) := \{v \in C^0(\bar{\mathcal{P}}) : v|_e \in \mathbb{P}_k(e) \forall e \subset \partial\mathcal{P}, \Delta v \in \mathbb{P}_\delta(\mathcal{P})\},$$

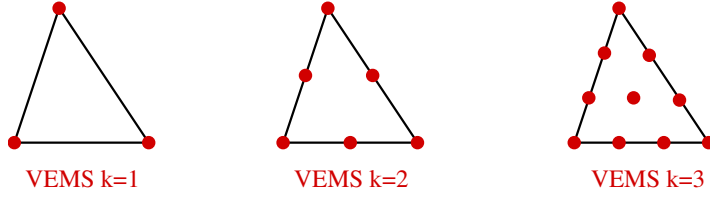


Fig. 4 Triangles: dofs for serendipity VEM

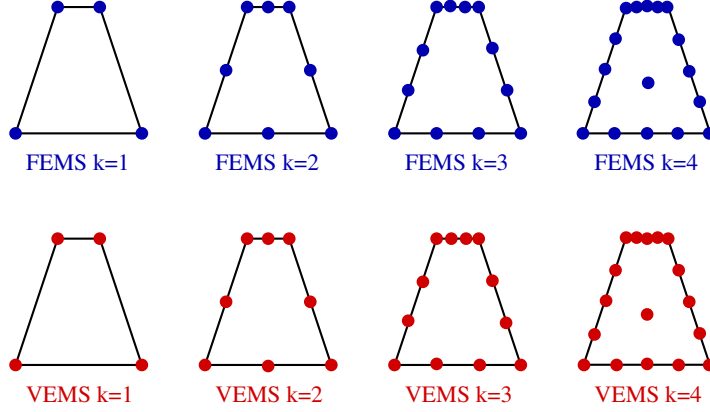


Fig. 5 Quads: dofs for serendipity FEM and VEM

with the degrees of freedom

$$(D_1) - (D_2) \quad \text{plus the moments of order up to } \delta : \int_{\mathcal{P}} v p_\delta dx \quad \forall p_\delta \in \mathbb{P}_\delta(\mathcal{P}).$$

Then, using the boundary dofs and the moments up to $k - 2$, we construct the Π_k^∇ operator as in (6), and use it (mimicking (14), with Π_k^∇ instead of Π_k) to define the moments of v of all orders between $k - 1$ and δ . Thus, the new space is

$$V_k^E(\mathcal{P}) := \left\{ v \in \tilde{V}_\delta^E(\mathcal{P}) \text{ s.t. } \int_{\mathcal{P}} v p_s dx = \int_{\mathcal{P}} \Pi_k^\nabla v p_s dx \quad \forall p_s \in \mathbb{P}_s^{hom}, k - 1 \leq s \leq \delta \right\}. \quad (15)$$

Remark 1 The advantage of the enhancement trick is that it can always be done, for every polygon \mathcal{P} , without recurring to a least-squares solution. On the other hand, the Serendipity approach becomes more and more powerful when the number of non-aligned edges of \mathcal{P} increases. For instance, on a decomposition made by non degenerate hexagons, the Serendipity VEM spaces of order k will have no internal degrees of freedom whenever $k \leq 5$. This of course will not be true for *degenerate* polygons, as for instance, in Fig. 1, for the leftmost example, where the first bubble appears for $k = 3$, and for the rightmost one, where the first bubble will appear for $k = 5$.

Remark 2 Serendipity FEM were introduced on quadrilaterals in order to reduce the number of internal degrees of freedom, and avoid the need for higher order numerical integration

schemes. For VEM, as we have seen, Serendipity elements are also convenient on triangles. But, in spite of the fact that we use the name ‘‘Serendipity’’ for both VEM and FEM, the spirit of the procedure is rather different from one case to the other. In the FEM context, the Serendipity approach is usually performed by: i) choosing the degrees of freedom that one wants to eliminate (typically, one or more internal node), and ii) choosing, accordingly (in general, kicking out one or more monomials), a polynomial subspace where the new, reduced set of degrees of freedom, is unisolvent. See for instance the classical [54] and the references therein, as well as the more evolved [3]. Instead in Serendipity VEM, as we have seen, we look first for a *projector*, onto the space of polynomials, that can be computed using a smaller number of degrees of freedom. Then we restrict ourselves to the subspace (of the original VEM space) where the values to be assigned to the other degrees of freedom (not used in constructing the projector) are taken from the values of the projector. See again [17].

Remark 3 One might argue that static condensation could be a simpler procedure to reduce the internal degrees of freedom. This is true in two dimensional problems, but it is not anymore the case for three dimensional problems, where the reduction of dofs on faces is important. Static condensation on faces might turn into a nightmare, while the serendipity approach works very well.

2.3 Non-conforming Virtual Elements

Another typical Finite Element variant of Galerkin approximations is given by the so-called Nonconforming methods, where the inclusion $V_h \subset H^1(\Omega)$ does not hold anymore, and the continuity across interelement boundaries is required only in a *weak sense* (typically, on each edge the average and the moments up to the order $k - 1$, where k is, as before, the order of the polynomials that we want to be included). See e.g. [29] and the references therein.

We just try to give the flavor of the Nonconforming Virtual Elements, referring for instance to [2, 12, 48, 53]. The local space is:

$$V_k^{NC}(\mathcal{P}) := \left\{ v \in H^1(\mathcal{P}) : \frac{\partial v}{\partial n}|_e \in \mathbb{P}_{k-1}(e) \forall \text{ edge } e, \Delta v \in \mathbb{P}_{k-2}(\mathcal{P}) \forall \mathcal{P} \right\}.$$

Before introducing the global space we need some notation. We introduce the space $H^1(\mathcal{T}_h) = \prod_{\mathcal{P} \in \mathcal{T}_h} H^1(\mathcal{P})$, and for $\varphi \in H^1(\mathcal{T}_h)$ we denote by $[[\varphi]]$ its jump on internal edges $e \in \mathcal{T}_h$. Then, the natural counterpart of (5), for $k \geq 1$ is now

$$V_h^{NC} := \left\{ v \in H^1(\mathcal{T}_h) : v|_{\mathcal{P}} \in V_k^{NC}(\mathcal{P}) \forall \mathcal{P}, \right. \\ \left. \int_e [[v]] p_{k-1} ds = 0 \forall \text{ internal edge } e, \forall p_{k-1} \in \mathbb{P}_{k-1}(e), \right. \\ \left. \int_e v p_{k-1} ds = 0 \forall e \text{ on } \partial\Omega, \forall p_{k-1} \in \mathbb{P}_{k-1}(e) \right\}.$$

The degrees of freedom are given by

$$(D'_1) : \text{ the moments } \int_e v p_{k-1} ds \quad \forall p_{k-1} \in \mathbb{P}_{k-1}(e) \quad \forall e, \\ (D'_2) : \text{ for } k \geq 2 \text{ the moments } \int_{\mathcal{P}} v p_{k-2} dx \quad \forall p_{k-2} \in \mathbb{P}_{k-2}(\mathcal{P}).$$

It is not difficult to see that these are indeed a set of degrees of freedom for V_h^{NC} . It is also easy to see that, using them, for every $v \in V_h^{NC}$ and for each polygon \mathcal{P} we can compute its ∇ -projection $\Pi_k^\nabla v$ defined as in (6). Using the Π_k^∇ operator as in (7) one can now construct the *local* as well as the *global* approximate bilinear form a_h . Then, basically, we deal with them as with usual nonconforming Finite Elements.

Just to give an idea of the possible comparison between nonconforming FEM and VEM, we consider the case of $k = 2$ on triangles. Both for FEM and VEM we take first as boundary degrees of freedom the moments, on each edge, of order ≤ 1 . But on triangles (and on quadrilaterals as well), since $k = 2$ is *even*, FEM also need an additional degree of freedom *inside*; indeed the six values at the 3×2 Gauss points do not identify a polynomial of degree ≤ 2 on the triangle in a unique way (take an ellipses through the six points and you get a $p_2 \neq 0$ that vanishes at all six points). VEM are not better off, since their internal degree of freedom cannot be eliminated through some sort of Serendipity trick, (exactly for the same reason: there is a p_2 that is orthogonal, on each edge, to all linear and to all constant functions). The typical escape for FEM is to add a seventh polynomial (see e.g. [33]): referring to Fig. 6, indicating with λ_A , λ_B , and λ_C the usual barycentric coordinates, we add

$$\zeta := \lambda_A \lambda_B (\lambda_A - \lambda_B) + \lambda_B \lambda_C (\lambda_B - \lambda_C) + \lambda_C \lambda_A (\lambda_C - \lambda_A) \quad (16)$$

and take *the mean value on \mathcal{P}* as seventh degree of freedom.

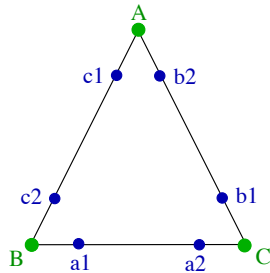


Fig. 6 Toward Nonconforming VEM

When using VEM we already have seven functions and the distinction between k *odd* or k *even* is not necessary. In some sense, the nonconforming VEM are already happy as they are, no matter whether k is even or odd. The difference is that for k *even* we could not play some smart Serendipity trick in order to get rid of some internal degrees of freedom, while this would be allowed for k *odd*. In the case $k = 2$ we see that the VEM space obviously contains all polynomials of degree ≤ 2 . The additional (non polynomial) element could be thought of as being generated by adding to the space \mathbb{P}_2 one function. For instance we can choose the VEM function, say $\chi(x, y)$, that, with the notation of Fig. 6, could be identified by the following conditions:

$$\begin{aligned} \int_{\mathcal{P}} \chi dx &= 0, & \int_e \chi ds &= 0 \quad \forall \text{ edge } e, \\ \frac{1}{|e_a|} \int_{e_a} \chi q_a ds &= \frac{1}{|e_b|} \int_{e_b} \chi q_b ds = \frac{1}{|e_c|} \int_{e_c} \chi q_c ds = 1, \end{aligned}$$

where: the edge e_a , with length $|e_a|$, is opposite to the vertex A , and q_a is the polynomial of degree 1 such that $q_a(a_1) = 1$ and $q_a(a_2) = -1$ (and similar notation for the edges e_b and e_c). We point out that on the boundary of our triangle the function χ cannot be the trace of a polynomial of degree ≤ 2 . Indeed, it is easy to check that every $v \in \mathbb{P}_2$ verifies

$$\frac{1}{|e_a|} \int_{e_a} v q_a ds + \frac{1}{|e_b|} \int_{e_b} v q_b ds + \frac{1}{|e_c|} \int_{e_c} v q_c ds = 0.$$

On the boundary the behaviour of χ is quite similar to that of ζ given in (16), but the normal derivative of χ is on each edge a polynomial of degree 1 (and not 2 as ζ) and (most important) $\Delta \chi$ is constant (instead of linear): a feature that might turn out to be convenient in certain problems where some equilibrium or conservation properties could be enforced strongly and not “only on average”.

2.4 Conforming VEM in 3 Dimensions

Let \mathcal{P} be a polyhedron, and let f be a face. We begin by defining the space

$$V_k(\mathcal{P}) := \left\{ v \in C^0(\overline{\mathcal{P}}) : v|_f \in V_k(f) \forall f \subset \partial \mathcal{P}, \Delta v \in \mathbb{P}_{k-2}(\mathcal{P}) \right\},$$

where $V_k(f)$ is the space defined in (3). The degrees of freedom will be

$$\begin{aligned} (D_1) &: \text{the values of } v \text{ at the vertices,} \\ (D_2) &: \text{for } k \geq 2 \text{ the moments } \int_e v p_{k-2} ds \quad \forall p_{k-2} \in \mathbb{P}_{k-2}(e) \quad \forall \text{ edge } e, \quad (17) \\ (D_3) &: \text{for } k \geq 2 \text{ the moments } \int_f v p_{k-2} dx \quad \forall p_{k-2} \in \mathbb{P}_{k-2}(f) \quad \forall \text{ face } f, \\ (D_4) &: \text{for } k \geq 2 \text{ the moments } \int_{\mathcal{P}} v p_{k-2} dx \quad \forall p_{k-2} \in \mathbb{P}_{k-2}(\mathcal{P}). \end{aligned}$$

Proceeding as we did before, the next step is to compute the Π_k^∇ operator as in (6). To this end, integrating by parts we obtain

$$\int_{\mathcal{P}} \nabla \Pi_k^\nabla v \cdot \nabla q_k := \int_{\mathcal{P}} \nabla v \cdot \nabla q_k = - \int_{\mathcal{P}} v \Delta q_k + \sum_{f \in \partial \mathcal{P}} \int_f v \frac{\partial q_k}{\partial n},$$

and we realize that the integrals on faces cannot be computed out of the dofs (17). Indeed, we would need moments of order $k-1$ and not just $k-2$. We then use the enhanced procedure explained in Section 2.2 (see (15)), and define the new space

$$\widetilde{V}_k(\mathcal{P}) := \left\{ v \in C^0(\overline{\mathcal{P}}) : v|_f \in V_k^E(f) \forall f \subset \partial \mathcal{P}, \Delta v \in \mathbb{P}_{k-2}(\mathcal{P}) \right\}.$$

We point out that the serendipity approach could be used on faces to reduce the number of dofs. We refer to [17] for details.

3 $H(\text{div})$ and $H(\text{rot})$ Conforming FEM/VEM on Triangles

3.1 FEM for $H(\text{div}; \Omega)$ and $H(\text{rot}; \Omega)$ Spaces

Similarly to what we did for VEM discretizations of H^1 we can now present the VEM discretizations of vector-valued spaces $H(\text{div}; \Omega)$ and $H(\text{rot}; \Omega)$. We recall that in Finite Elements we have, essentially, *two families* of spaces for $H(\text{div}; \Omega)$ that go under the name of *Raviart–Thomas* [51] and *Brezzi–Douglas–Marini* [21] (in short: RT and BDM), and *two families* of spaces for $H(\text{rot}; \Omega)$ that go under the name of *Nédélec of first kind* [49] and *Nédélec of second kind* [50] (in short: N1 and N2). We recall them here below, for triangular elements: For k integer

$$RT_k := \{(\mathbb{P}_k)^2 + \mathbf{x}\mathbb{P}_k\}, \quad N1_k := \{(\mathbb{P}_k)^2 + \mathbf{x}^\perp\mathbb{P}_k\}, \quad k \geq 0$$

and

$$BDM_k \equiv N2_k := (\mathbb{P}_k)^2, \quad k \geq 1.$$

The *boundary degrees of freedom* are, for all edge e :

$$\begin{aligned} \int_e \mathbf{v} \cdot \mathbf{n} q_k ds \quad \forall q_k \in \mathbb{P}_k(e) \quad \text{for } RT_k \text{ and } BDM_k, \\ \int_e \mathbf{v} \cdot \mathbf{t} q_k ds \quad \forall q_k \in \mathbb{P}_k(e) \quad \text{for } N1_k \text{ and } N2_k. \end{aligned}$$

The *internal degrees of freedom* are, for $k \geq 1$ and for all triangles T ,

$$\text{For } RT_k : \int_T \mathbf{v} \cdot \mathbf{q} dx \quad \forall \mathbf{q} \in BDM_{k-1} \quad \text{and for } BDM_k : \int_T \mathbf{v} \cdot \mathbf{q} dx \quad \forall \mathbf{q} \in N1_{k-2} \quad (18)$$

as well as

$$\text{For } N1_k : \int_T \mathbf{v} \cdot \mathbf{q} dx \quad \forall \mathbf{q} \in N2_{k-1} \quad \text{and for } N2_k : \int_T \mathbf{v} \cdot \mathbf{q} dx \quad \forall \mathbf{q} \in RT_{k-2}. \quad (19)$$

Clearly, for $k = 1$ both RT_{k-2} and $N1_{k-2}$ are empty, and the corresponding dofs (in (18) and in (19), respectively) are not there.

For the three-dimensional case, as well as for the case of quadrilaterals and hexahedra, where, however, the definitions are less straightforward, we refer for instance to [20–23] or to [4].

Moreover, for the two dimensional case on triangles, we remark the perfect symmetry between the $H(\text{div}; T)$ and the $H(\text{rot}; T)$ case: changing \mathbf{n} with \mathbf{t} as well as **grad** with **rot** and **div** with **rot**. Hence, from now on, in this section we will restrain ourselves to the case of $H(\text{div}; \mathcal{P})$ spaces on triangles.

3.2 VEM $H(\text{div}; \mathcal{P})$ Spaces on Triangles

Here too we still have to distinguish between *RT-like* and *BDM-like* spaces: roughly speaking, for $\mathbf{v} \cdot \mathbf{n}$ a polynomial of order k on the boundary, we will have spaces having the divergence in \mathbb{P}_k (the RT case, for $k \geq 0$) and spaces having the divergence in \mathbb{P}_{k-1} (the BDM case, for $k \geq 1$). We refer to [22] and [16] for more details.

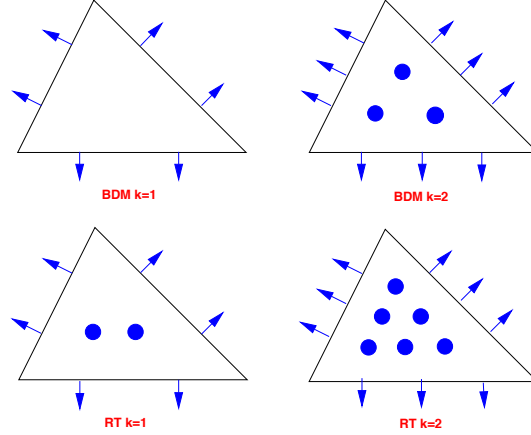


Fig. 7 Face FEM, $k = 1$ and $k = 2$

On a (general) polygon \mathcal{P} , for $k = \text{degree of } \mathbf{v} \cdot \mathbf{n}$ on each edge, and $\delta = \text{degree of the divergence (equal to } k \text{ or } k - 1)$ we set

$$V_{k,\delta}(\mathcal{P}) := \{ \mathbf{v} \in H(\text{div} : \mathcal{P}) \cap H(\text{rot} : \mathcal{P}) \text{ s.t. } \mathbf{v} \cdot \mathbf{n}|_e \in \mathbb{P}_k(e) \forall e, \\ \text{div } \mathbf{v} \in \mathbb{P}_\delta(\mathcal{P}), \text{rot } \mathbf{v} \in \mathbb{P}_{k-1}(\mathcal{P}) \}.$$

The degrees of freedom in $V_{k,\delta}(\mathcal{P})$ are

- $(D_1) \int_e \mathbf{v} \cdot \mathbf{n} q_k ds \quad \forall q_k \in \mathbb{P}_k(e) \quad \forall \text{edge } e \text{ in } \partial \mathcal{P},$
- $(D_2) \text{ (for } k > 0 \text{ and } \delta > 0) \int_{\mathcal{P}} \mathbf{v} \cdot \mathbf{grad} q_\delta dx \quad \forall q_\delta \in \mathbb{P}_\delta(\mathcal{P}),$
- $(D_3) \text{ (for } k > 0) \int_{\mathcal{P}} \text{rot } \mathbf{v} q_{k-1} dx \quad \forall q_{k-1} \in \mathbb{P}_{k-1}(\mathcal{P}).$

See Fig. 8 where the blue d.o.f.s are common to FEM and VEM, and the green ones are the additional dofs needed for VEM.

A comparison with FEM shows that, as in the scalar case, VEM exhibit more internal dofs: one more for $k = 1$ (the green bullet), and three more for $k = 2$. As we did for scalar approximations (see (14) and (15)), they could be eliminated by the *enhancement* or by the *serendipity* approaches. See e.g. [18].

Considering again the simplest case, here $k = 1$, we see that the additional degree of freedom corresponds to the addition (to the FEM space BDM_1 or RT_1) of $\mathbf{rot} \beta_2$, where β_2 is the function defined in (10). For $k = 2$, at first sight we could think that we are adding, to the FEM space, the \mathbf{rot} of the three functions β_3 such that $\beta_3 = 0$ on $\partial \mathcal{P}$ and $\Delta \beta_3 \in \mathbb{P}_1$. There are three independent ones, but on a triangular domain one of them is the cubic bubble, whose \mathbf{rot} is already in the BDM_2 space as well as in the RT_2 space. Hence, we are just adding *two* new ones to the FEM case (see the green dots in Fig. 8).

Here too, we point out that for VEM the passage from triangles to quadrilaterals (of *very general* shape) is immediate (as well as the passage to more general polygons), while the FEM spaces, already for quadrilaterals, and more on hexahedra, require a considerable additional work. See for instance [8] and the references therein.

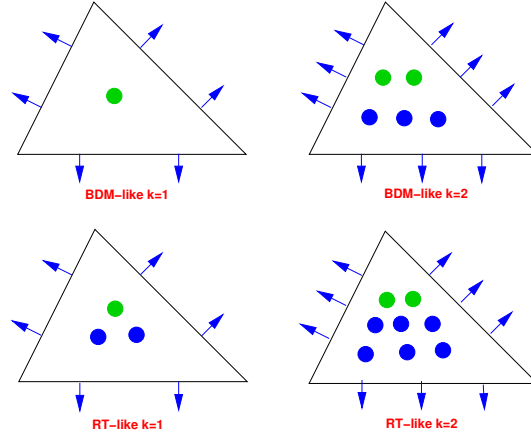


Fig. 8 Face VEM $k = 1$ and $k = 2$

4 C^p VEM for $p \geq 1$

With Virtual Elements it is quite easy to construct high-regularity approximations. Here we shall deal mostly with C^1 approximations, having in mind, as an example of fourth order problem, a plate bending problem:

$$D\Delta^2 w = f \text{ in } \Omega, \quad w = \frac{\partial w}{\partial n} \text{ on } \partial\Omega,$$

where D is the bending rigidity. The variational formulation looks like (1), with $V = H_0^2(\Omega)$, and

$$a(v, w) = D \left[(1 - \nu) \int_{\Omega} w_{/ij} v_{/ij} dx + \nu \int_{\Omega} \Delta w \Delta v dx \right], \quad \langle f, v \rangle = \int_{\Omega} f v dx. \quad (20)$$

In (20) ν is the Poisson's ratio, $v_{/i} = \partial v / \partial x_i$, $i = 1, 2$, and we used the summation convention of repeated indices. Throughout this section $w_{/n}$ will denote the normal derivative, $w_{/t}$ the tangential derivative in the counterclockwise ordering of the boundary, and so on. When no confusion occurs we might also use w_n, w_t, \dots . As we said, we will concentrate on C^1 elements. But at the end of this section we will give a hint on C^p elements for $p \geq 2$.

4.1 C^1 -elements

The possibilities of constructing C^1 -elements with the VEM approach are almost endless. To fix the ideas we will recall the approach given in [24, 26]. Let \mathcal{P} be a generic polygon in \mathcal{T}_h . For given integers $r \geq 0$, $s \geq 0$ and $m \geq -1$ we consider the space

$$V_{r,s,m}(\mathcal{P}) := \{w \in H^2(\mathcal{P}) : w|_e \in \mathbb{P}_r(e) \text{ and } w_{n|e} \in \mathbb{P}_s(e) \forall \text{ edge } e, \Delta^2 w \in \mathbb{P}_m \text{ in } \mathcal{P}\}. \quad (21)$$

Clearly, for the above space to have some sense, and for allowing the construction of H^2 spaces on the whole domain Ω , we need adding some restriction. In the vertices of the

decompositions we will need our spaces to be continuous with their first derivatives. This would require to have as degrees of freedom in each \mathcal{P}

- (D_0) the values of $w, w_{/1}$ and $w_{/2}$ at the vertices,

and in practice this will require, in a natural way, that

$$r \geq 3, \quad s \geq 1.$$

Moreover, we would need to have the traces of w and of $w_{/n}$ to be single-valued on edges. This will require to take as additional degrees of freedom

- (D_1) for $r \geq 4$, the moments $\int_e w q_{r-4} ds \quad \forall q_{r-4} \in \mathbb{P}_{r-4}(e), \quad \forall e \in \partial\mathcal{P}$,
- (D_2) for $s \geq 2$, the moments $\int_e w_{/n} q_{s-2} dx \quad \forall q_{s-2} \in \mathbb{P}_{s-2}(e), \quad \forall e \in \partial\mathcal{P}$.

Finally we will have as *internal* degrees of freedom

- (D_3) for $m \geq 0$, the moments $\int_{\mathcal{P}} w q_m dx \quad \forall q_m \in \mathbb{P}_m$.

The smallest space will then correspond to $r = 3, s = 1, m = -1$, and is an extension to polygons of the *reduced Hsieh–Clough–Tocher* composite triangular element (see for instance, [29]). The VEM space (for a general polygon \mathcal{P}) will then be

$$V(\mathcal{P}) := \{w \in H^2(\mathcal{P}) : w|_e \in \mathbb{P}_3(e), w_{n|e} \in \mathbb{P}_1(e) \quad \forall \text{ edge } e, \text{ and } \Delta^2 w = 0 \text{ in } \mathcal{P}\},$$

whose degrees of freedom are only the values of w and of its two derivatives at the vertices of \mathcal{P} , that is, (D_0) . See Fig. 9.

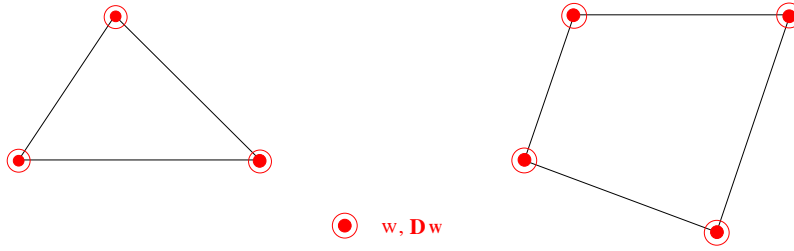


Fig. 9 C^1 VEM, reduced HCT-like

Another example (for $r = 3, s = 2, m = -1$) is given in Fig. 10; the corresponding element will have (D_0) and (D_2) as degrees of freedom and is a sort of VEM counterpart of the original *Hsieh–Clough–Tocher* composite triangular element (see again [29]).

In general, the space (21) will contain all polynomials \mathbb{P}_κ for

$$\kappa = \min\{r, s + 1, m + 4\} \quad (\equiv \text{order of precision})$$

and out of the degrees of freedom $(D_0), \dots, (D_3)$, (integrating by parts twice) we can compute an operator $\Pi_\kappa^{\mathcal{P}} : V_{r,s,m}(\mathcal{P}) \rightarrow \mathbb{P}_\kappa(\mathcal{P})$ defined on each element by

$$a^{\mathcal{P}} \left(\Pi_\kappa^{\mathcal{P}} v - v, q_\kappa \right) = 0 \quad \forall q_\kappa \in \mathbb{P}_\kappa(\mathcal{P}), \quad \int_{\partial\mathcal{P}} \left(\Pi_\kappa^{\mathcal{P}} v - v \right) q_1 ds = 0 \quad \forall q_1 \in \mathbb{P}_1(\mathcal{P}).$$

The discrete bilinear form, for v_h and w_h in $V_{r,s,m}(\mathcal{P})$, is then defined as in (7)

$$a_h^{\mathcal{P}}(v_h, w_h) := a^{\mathcal{P}}\left(\Pi_{\kappa}^{\mathcal{P}} v_h, \Pi_{\kappa}^{\mathcal{P}} w_h\right) + S^{\mathcal{P}}\left(\left(I - \Pi_{\kappa}^{\mathcal{P}}\right) v_h, \left(I - \Pi_{\kappa}^{\mathcal{P}}\right) w_h\right)$$

with $S^{\mathcal{P}}(v_h, w_h)$ taken, for instance, as in (8), provided that the dofs (D_0) – (D_3) are properly treated in order to scale all of them in the same way. For the treatment of the right-hand side and for the error estimates we refer to [24,26].

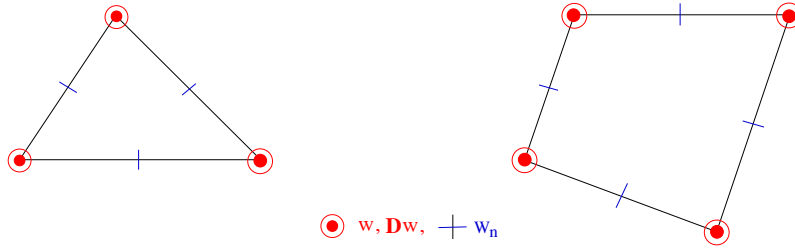


Fig. 10 C^1 VEM, HCT-like

Following a similar path, without any effort, and still on general polygons, we can design a huge variety of methods. See, for instance, Fig. 11, corresponding to the case $\kappa = 3$ ($r = 4$, $s = 3$, $m = -1$), where the degrees of freedom are those of Fig. 10 plus the value (at the midpoint of every edge) of w and of $w_{/n}$.

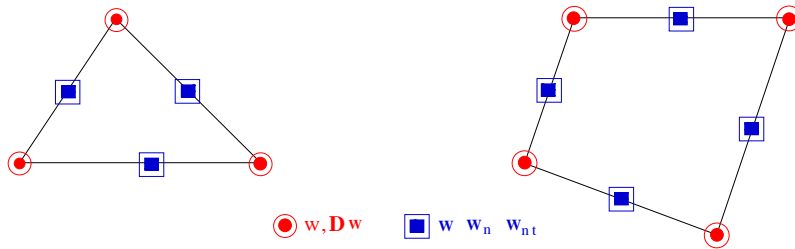


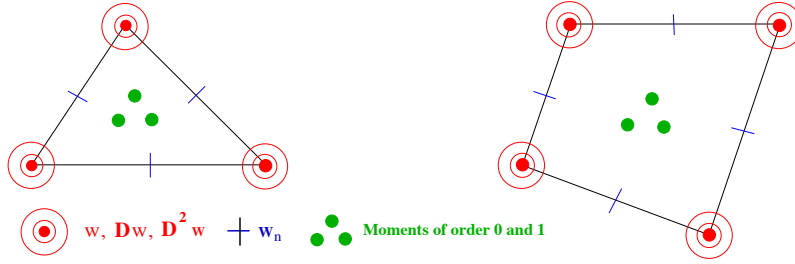
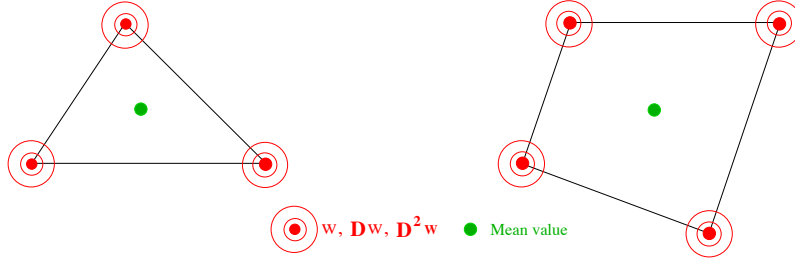
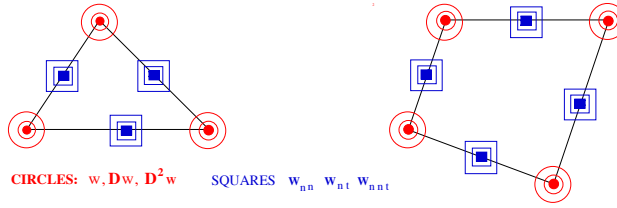
Fig. 11 C^1 VEM, Quartic w and cubic $w_{/n}$

If one wants to put as many degrees of freedom as possible on vertices (less numerous than edges) one can consider the *Argyris-like* elements of Figs. 12 and 13.

Comparing with their FEM analogues, we see that we have here some additional internal degrees of freedom. However, these could be easily eliminated by adapting the Serendipity/Enhancement approach described in Subsection 2.2 for C^0 VEM.

4.2 A Hint on C^p VEM for $p \geq 2$

Along the same lines, still for general polygons, we might easily construct C^p elements for $p \geq 2$. Just to give an example, we might consider the elements of Fig. 14 (where we also indicate the degrees of freedom).

Fig. 12 C^1 VEM, Quintic w and quartic w/n Fig. 13 C^1 VEM, Quintic w and cubic w/n Fig. 14 Examples of C^2 elements

In particular, Fig. 14 refers to the local spaces

$$V(\mathcal{P}) := \{v \in H^3(\mathcal{P}) : v|_e \in \mathbb{P}_5(e), v_n|_e \in \mathbb{P}_4(e), v_{nn}|_e \in \mathbb{P}_3(e) \forall e \in \partial\mathcal{P}, \Delta^3 v = 0 \text{ in } \mathcal{P}\}.$$

Out of the degrees of freedom we can once more compute an operator $\Pi_5^{\mathcal{P}} : V(\mathcal{P}) \rightarrow \mathbb{P}_5(\mathcal{P})$ defined by

$$\int_{\mathcal{P}} \left(D^3 \left(\Pi_5^{\mathcal{P}} v - v \right) \right) : (D^3 q_5) dx = 0 \quad \forall q_5 \in \mathbb{P}_5, \quad \int_{\partial\mathcal{P}} \left(\Pi_5^{\mathcal{P}} v - v \right) q_2 ds = 0 \quad \forall q_2 \in \mathbb{P}_2(\mathcal{P}).$$

The discrete bilinear form is then constructed as before as

$$a_h^{\mathcal{P}}(v_h, w_h) := a^{\mathcal{P}} \left(\Pi_5^{\mathcal{P}} v_h, \Pi_5^{\mathcal{P}} w_h \right) + S^{\mathcal{P}} \left(\left(I - \Pi_5^{\mathcal{P}} \right) v_h, \left(I - \Pi_5^{\mathcal{P}} \right) w_h \right) \quad v_h, w_h \in V(\mathcal{P}),$$

with $S^{\mathcal{P}}(v_h, w_h)$ taken, for instance, again as in (8).

Remark 4 A family of nonconforming elements for plates was introduced independently in [2,53], which we refer to for a detailed description.

Remark 5 As a general consideration, we underline the fact that, in particular for two-dimensional cases, the construction of Virtual Element spaces is extremely easy: one should only set the degrees of freedom (for the function and the normal derivatives) on each edge. The edges being one-dimensional, this is elementary.

Remark 6 On the other side, we must also point the attention to the fact that, so far, the choice of a convenient stabilization procedure seems here to be less easy than for other cases. To be more precise: it is not difficult to construct stabilising bilinear forms that make the discrete problem well posed. However, in many cases the guidelines for an optimal choice of the “stabilizing parameters” in front of them, or in front of some individual pieces of them, is far from clear. Just to make an example, the HCT-like element of Fig. 10 can be easily stabilised with, essentially, any of the different strategies used for C^0 elements. But this is not the case for its reduced-HCT-like companion of Fig. 9. In each particular case a suitable choice of the stabilising parameter can be (relatively) easily found by trial and error, but... *this is not what we like*. At a more general level we feel that a novel point of view should be found, allowing the determination of clear guidelines for the choice of stabilising terms. Indeed, in our opinion, this is possibly the weakest point of VEM in general, and all new points of view would be *more than welcome!*

5 VEM for Stokes and Incompressible Elasticity

5.1 Stokes 2D

We recall (to set the notation) the incompressible Stokes equations for a polygon Ω with homogeneous Dirichlet boundary conditions, and forcing term $\mathbf{f} \in (L^2(\Omega))^2$:

Find $\mathbf{u} \in (H_0^1(\Omega))^2$ and $p \in L^2(\Omega)$ such that:

$$\begin{aligned} -\Delta \mathbf{u} + \nabla p &= \mathbf{f} && \text{in } \Omega, \\ \operatorname{div} \mathbf{u} &= 0 && \text{in } \Omega. \end{aligned} \quad (22)$$

Setting: $\mathbf{V} := (H_0^1(\Omega))^2$, $Q := L_0^2(\Omega)$ ($= L^2$ functions with zero mean value), and

$$a(\mathbf{u}, \mathbf{v}) := \int_{\Omega} \boldsymbol{\varepsilon}(\mathbf{u}) : \boldsymbol{\varepsilon}(\mathbf{v}) d\Omega \quad \forall \mathbf{u}, \mathbf{v} \in \mathbf{V}, \quad b(\mathbf{v}, q) := \int_{\Omega} \operatorname{div} \mathbf{v} q d\Omega \quad \forall \mathbf{v} \in \mathbf{V}, \forall q \in Q,$$

where $\boldsymbol{\varepsilon}(\mathbf{v}) = (\nabla \mathbf{v} + (\nabla \mathbf{v})^T)/2$ is the symmetric gradient, the variational formulation of the problem can be written as: Find $\mathbf{u} \in \mathbf{V}$, $p \in Q$ such that

$$\begin{cases} a(\mathbf{u}, \mathbf{v}) + b(\mathbf{v}, p) = (\mathbf{f}, \mathbf{v}) & \forall \mathbf{v} \in \mathbf{V}, \\ b(\mathbf{u}, q) = 0 & \forall q \in Q. \end{cases} \quad (23)$$

Remark 7 From a purely mathematical point of view, as it is well known, the equations in (23) coincide, up to the aspects related to the material properties, with the ones of incompressible elasticity in the mixed (\mathbf{u}, p) . formulation. Hence the title of this section, where, indeed, we will limit ourselves to the discussion of the Stokes case alone.

Remark 8 For the sake of simplicity we will keep the viscosity coefficient equal to 1, and we will stick to the (widely unrealistic) case of homogeneous Dirichlet boundary conditions on the whole boundary $\partial\Omega$, as it is (quite often) done in the Mathematical literature.

Taking a sequence of conforming discretizations of this problem with $\mathbf{V}_h \subset \mathbf{V}$ and $Q_h \subset Q$, and suitable approximations a_h and b_h of the bilinear forms a and b , respectively, one can write the discretized version as: Find $\mathbf{u}_h \in \mathbf{V}_h$ and $p_h \in Q_h$ such that

$$\begin{cases} a_h(\mathbf{u}_h, \mathbf{v}_h) + b_h(\mathbf{v}_h, p_h) = (\mathbf{f}_h, \mathbf{v}_h) & \forall \mathbf{v}_h \in \mathbf{V}_h, \\ b_h(\mathbf{u}_h, q_h) = 0 & \forall q_h \in Q_h, \end{cases} \quad (24)$$

where, in turn, \mathbf{f}_h is (if needed) a suitable approximation of \mathbf{f} . It is well known that convergence of the method with optimal error bounds relies on the *inf-sup* stability condition

$$\exists \beta > 0 \text{ such that } \inf_{q_h \in Q_h} \sup_{\mathbf{v}_h \in \mathbf{V}_h} \frac{b(\mathbf{v}_h, q_h)}{\|\mathbf{v}_h\|_V \|q_h\|_Q} \geq \beta \quad \forall h. \quad (25)$$

A huge number of different *stable pairs* pairs (\mathbf{V}_h, Q_h) satisfying (25) can be found in the FEM literature. We refer, for simplicity, to [20] and the references therein. Once a stable pair has been chosen, one can wonder whether the resulting solution \mathbf{u}_h would satisfy *exactly*

$$\operatorname{div} \mathbf{u}_h \equiv 0 \quad \text{in } \Omega, \quad (26)$$

a condition that would be of considerable help in the mathematical treatment of the discretized problem, and, most important, would be quite relevant from the physical point of view (ensuring the exact incompressibility of the discrete solution). Clearly this (for conforming approximations) will hold if, in every element \mathcal{P} of the decomposition, we had that

$$\left\{ \{\mathbf{u}_h \in \mathbf{V}_h\} \text{ and } \left\{ \int_{\mathcal{P}} \operatorname{div} \mathbf{u}_h q_h dx = 0 \quad \forall q_h \in Q_h \right\} \right\} \Rightarrow \{\operatorname{div} \mathbf{u}_h = 0 \text{ in } \mathcal{P}\}. \quad (27)$$

A simple (and rather natural) sufficient condition for (27) is clearly

$$\operatorname{div}\{\mathbf{V}_h\} \subseteq Q_h$$

that however, joined with (25), would imply

$$\operatorname{div}\{\mathbf{V}_h\} \equiv Q_h, \quad (28)$$

a rather stringent requirement, verified only with very few (and somehow rather cumbersome) choices of discretizations (and in general only for special types of decompositions). Among the many recent papers on Finite Element discretizations of the problem we mention [27, 28, 32, 34, 39, 37, 38, 40, 41, 52] and refer especially to the excellent review [47], and to the references therein.

Let us see how to design divergence-free Virtual Elements on practically arbitrary grids. We concentrate on the 2D case, and refer to the results in [19].

For the velocity space we look first at the boundary, and we define, for $k \geq 2$ and for a polygon \mathcal{P} , the space

$$\mathcal{B}_k(\partial\mathcal{P}) := \{\mathbf{v} \in (C^0(\partial\mathcal{P}))^2 \text{ s.t. } \mathbf{v}|_e \in (\mathbb{P}_k(e))^2 \quad \forall \text{ edge } e \text{ of } \partial\mathcal{P}\}. \quad (29)$$

Clearly, the dimension of $\mathcal{B}_k(\partial\mathcal{P})$ for a polygon with n edges would be

$$\dim \mathcal{B}_k(\partial\mathcal{P}) = 2nk.$$

Then we can define the VEM space for velocities:

$$\mathcal{V}_k(\mathcal{P}) := \{\mathbf{v} \in (H^1(\mathcal{P}))^2 \text{ s.t. } \mathbf{v}|_{\partial\mathcal{P}} \in \mathcal{B}_k(\partial\mathcal{P}), \operatorname{rot}(\Delta\mathbf{v}) \in \mathbb{P}_{k-3}, \operatorname{div} \mathbf{v} \in \mathbb{P}_{k-1}\}, \quad (30)$$

while for the pressure we simply take

$$Q_k(\mathcal{P}) = \mathbb{P}_{k-1}(\mathcal{P}).$$

The dimension of $\mathcal{V}_k(\mathcal{P})$ is then equal to $2nk$ (dimension of $\mathcal{B}_k(\partial\mathcal{P})$) plus π_{k-3} , plus $\pi_{k-1} - 1$ (since, from Gauss theorem, the mean value of the divergence is determined already by the boundary values). Then

$$\dim \mathcal{V}_k(\mathcal{P}) = 2nk + \frac{(k-2)(k-1)}{2} + \frac{k(k+1)}{2} - 1 = 2nk + k^2 - k.$$

Accordingly, one can show (see [19]) that a set of degrees of freedom for $\mathcal{V}_k(\mathcal{P})$ can be taken as

- the values of \mathbf{v} at the n vertices ($= 2n$ dofs),
- the values of \mathbf{v} at $k-1$ distinct points inside each edge ($= 2n(k-1)$ dofs),
- the values of $\int_{\mathcal{P}} \mathbf{v} \cdot \mathbf{x}^\perp q_{k-3} ds$ for every $q_{k-3} \in \mathbb{P}_{k-3}$,
- the values of $k(k+1)/2 - 1$ moments of $\operatorname{div} \mathbf{v}$.

The degrees of freedom for Q_k , in each element, will be equal to π_{k-1} internal moments.

It can be shown (see always [19]) that, using the above degrees of freedom, for each $\mathbf{v} \in \mathcal{V}_k(\mathcal{P})$ one can compute, among other things, its divergence (which is a polynomial), and also compute the operator $\Pi_k^\varepsilon : \mathcal{V}_k(\mathcal{P}) \rightarrow (\mathbb{P}_k(\mathcal{P}))^2$ defined by

$$\begin{cases} \int_{\mathcal{P}} \boldsymbol{\varepsilon}(\mathbf{v} - \Pi_k^\varepsilon \mathbf{v}) : \boldsymbol{\varepsilon}(\mathbf{q}_k) dx = 0 & \forall \mathbf{q}_k \in (\mathbb{P}_k)^2, \\ \int_{\partial\mathcal{P}} (\mathbf{v} - \Pi_k^\varepsilon \mathbf{v}) ds = \mathbf{0} \end{cases}$$

that, in turn, allows to define, on each element \mathcal{P} , a discrete bilinear form:

$$a_h^{\mathcal{P}}(\mathbf{u}, \mathbf{v}) := \int_{\mathcal{P}} \boldsymbol{\varepsilon}(\Pi_k^\varepsilon \mathbf{u}) : \boldsymbol{\varepsilon}(\Pi_k^\varepsilon \mathbf{v}) dx + S^{\mathcal{P}}(\mathbf{u} - \Pi_k^\varepsilon \mathbf{u}, \mathbf{v} - \Pi_k^\varepsilon \mathbf{v}) \quad \forall \mathbf{u}, \mathbf{v} \in \mathcal{V}_k(\mathcal{P}),$$

where $S^{\mathcal{P}}$ is again one of the common *stabilizing* bilinear forms of VEM theory, as for instance the analogue of the one in (8).

The discrete bilinear form a_h will then be obtained by summing the contributions of all the polygons \mathcal{P} . On the other hand, the bilinear form $b(\mathbf{v}, q)$ is directly computable, for every $\mathbf{v} \in \mathcal{V}_k(\mathcal{P})$ and $q \in Q_k(\mathcal{P})$, using the degrees of freedom. Finally, for the right-hand side we use $\Pi_{k-2}^0 \mathbf{f}$ instead of \mathbf{f} , as we did in (9)).

Setting

$$\begin{aligned} \mathbf{V}_h &= \{\mathbf{v} \in \mathbf{V} : \mathbf{v}|_{\mathcal{P}} \in \mathcal{V}_k(\mathcal{P}) \forall \mathcal{P} \in \mathcal{T}_h\}, \\ Q_h &= \left\{ q \mid q|_{\mathcal{P}} \in Q_k(\mathcal{P}) \forall \mathcal{P} \in \mathcal{T}_h, \text{ and } \int_{\Omega} q = 0 \right\}, \end{aligned}$$

we have now all the ingredients that define the discrete problem:

Find $\mathbf{u}_h \in \mathbf{V}_h$, $p_h \in Q_h$ such that

$$\begin{cases} a_h(\mathbf{u}_h, \mathbf{v}_h) + b(\mathbf{v}_h, p_h) = (\Pi_{k-2}^0 \mathbf{f}, \mathbf{v}_h) & \forall \mathbf{v}_h \in \mathbf{V}_h, \\ b(\mathbf{u}_h, q_h) = 0 & \forall q_h \in Q_h. \end{cases} \quad (31)$$

The following figures show the degrees of freedom for $k=2$ and $k=3$ on triangles and quads. The squares correspond to *vectorial* degrees of freedom (so, they amount to 2 dofs each).

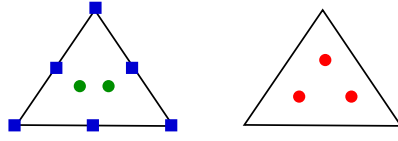


Fig. 15 Dofs for $k = 2$, on triangles, for velocities (left) and pressures (right)

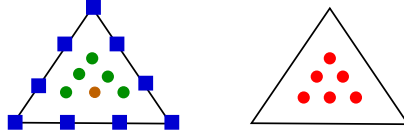


Fig. 16 Dofs for $k = 3$, on triangles, for velocities (left) and pressures (right)

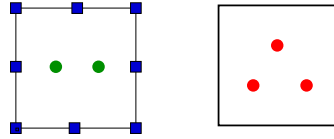


Fig. 17 Dofs for $k = 2$, on quads, for velocities (left) and pressures (right)

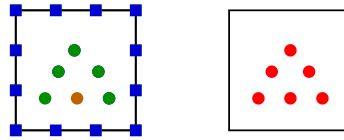


Fig. 18 Dofs for $k = 3$, on quads, for velocities (left) and pressures (right)

It is important, in our opinion, to point out once more that, apart from the number n of edges (and consequently the dimension of \mathcal{B}_k), nothing changes when passing from triangles to quads. And nothing would change passing to more general polygons.

It is not (at all!) easy, now, to compare VEM with FEM on triangles, due to the abundance of different Finite Element approaches that appeared in the literature since the 70s. For a panorama of the different choices we refer again to the recent overview [47] and to the references therein. In order to show at least *one* comparison we decided to go for the (possibly) most well known triangular element, that is the Crouzeix–Raviart element [30].

And indeed, in our opinion, the comparison with the Crouzeix–Raviart pair is particularly clarifying. We recall that, in more detail, for the Crouzeix–Raviart element the space of velocities is made, in each triangle, of vector-valued quadratic velocities augmented by two cubic bubbles (one per component), and the space of pressures is made of piecewise linear (discontinuous) polynomials. It is well known (see, e.g. [30] or [20]) that the *inf-sup* property (25) is verified, while the divergence-free condition (26) does not hold, as the divergence of the velocity field will come out to be, in each element, a polynomial of degree 2 orthogonal to all linear polynomials but not necessarily equal to zero. Instead the VEM-pair of Fig. 15, which exhibits the same number of d.o.f.s of the Crouzeix–Raviart pair, produces a discrete solution which is *exactly* divergence-free. Indeed, the VEM velocity space can be thought of as obtained by adding to $(\mathbb{P}_2)^2$ two bubble-functions $\beta^{(i)}$ ($i = 1, 2$) solutions of the local Stokes problems:

Find $\boldsymbol{\beta}^{(i)} \in (H_0^1(\mathcal{P}))^2$ and $p^{(i)} \in L^2(\mathcal{P})$ such that

$$\begin{cases} -\Delta \boldsymbol{\beta}^{(i)} + \nabla p^{(i)} = \mathbf{0}, \\ \operatorname{div} \boldsymbol{\beta}^{(i)} = (\mathbf{x} - \mathbf{b})_i \end{cases} \quad (32)$$

for $i = 1, 2$ where $\mathbf{b} = (b_1, b_2)$ is the barycenter of \mathcal{P} .

On the same order of ideas, taking (for super-simplicity) the quadrilateral domain $\mathcal{Q} \equiv]-1, 1[\times]-1, 1[$, and again $k = 2$, we remark first that the space \mathcal{B}_2 as defined in (29) has obviously dimension 16, and can be thought of as being the direct sum of

- $\{\mathbb{P}_2\}_{|\partial\mathcal{Q}}^2$ (= the traces of $(\mathbb{P}_2)^2$ on $\partial\mathcal{Q}$. Note that this includes also the trace of x^2y^2 which actually coincides with the trace of $x^2 + y^2 - 1$ on $\partial\mathcal{Q}$),
- the space generated (for each component) by the traces of x^2y and of xy^2 ,

whose dimensions are clearly 12 and 4, respectively. The whole space $\mathcal{Q}_2(\mathcal{Q})$ can be seen as generated by the spaces above, plus the two velocity fields $(x^2y^2, 0)$ and $(0, x^2y^2)$ (for a total number of 18 unknowns, as obvious). Now the space of **traces** of the VEM Velocity fields coincides with that of **traces** of $\mathcal{Q}_2(\mathcal{Q})$ and has dimension 16 as well. To obtain the VEM spaces one can

- begin from the 12 vectors in $(\mathbb{P}_2)^2$ (that belong to both spaces, and that we would never give up!);
- then add the four vectors that have the same traces as $(x^2y, 0)$, $(0, x^2y)$, $(xy^2, 0)$, and $(0, xy^2)$, zero divergence, and each component with constant Laplacian.

We have a dimension 16 so far. We can now

- add the two solutions of equations (32), this time on the domain \mathcal{Q} .

The final dimension is now 18, in agreement with Fig. 17.

5.2 The Reduced VEM Spaces

An important variant of the VEM spaces for Stokes is given by the reduced VEM spaces for incompressible fluids. From a purely mathematical point of view it is clear that equation (22) is just a particular case of a more general “ $\operatorname{div} \mathbf{u} = g$ ” with g given in $L^2(\Omega)$ with zero mean value (or with a mean value compatible with the boundary values prescribed for \mathbf{u} , if these are different from zero).

In practice, however, the case of incompressible fluids (where, in other words $g \equiv 0$) occurs quite often in a number of important applications, so that it might deserve an *ad hoc* treatment.

When using VEM one can make profit of the property (28) of these spaces, and combine it with the perfectly incompressible case. This, in other words, will amount to consider, in each subdomain, instead of (30) the smaller choice

$$\mathcal{V}_k^r(\mathcal{P}) := \{ \mathbf{v} \in (H^1(\mathcal{P}))^2 \text{ s.t. } \mathbf{v}|_{\partial\mathcal{P}} \in \mathcal{B}_k(\partial\mathcal{P}), \operatorname{rot}(\Delta \mathbf{v}) \in \mathbb{P}_{k-3}, \operatorname{div} \mathbf{v} \in \mathbb{P}_0 \} \quad (33)$$

(whose dimension would just be $2nk + (k-2)(k-1)/2$), and take $\mathcal{Q}_0(\mathcal{P}) = \mathbb{P}_0(\mathcal{P})$. Starting from the local spaces one can then define the *global spaces* $\mathbf{V}_h^r \subset \mathbf{V}$, and $\mathcal{Q}_h^0 =$ piecewise constants, in the usual way. We can then consider the **reduced problem**: find $\mathbf{u}_h^r \in \mathbf{V}_h^r$ and $p_h^0 \in \mathcal{Q}_h^0$ such that

$$\begin{cases} a_h(\mathbf{u}_h^r, \mathbf{v}_h^r) + b(\mathbf{v}_h^r, p_h^0) = (\Pi_{k-2}^0 \mathbf{f}, \mathbf{v}_h^r) & \forall \mathbf{v}_h^r \in \mathbf{V}_h^r, \\ b(\mathbf{u}_h^r, q_h^0) = 0 & \forall q_h^0 \in \mathcal{Q}_h^0. \end{cases} \quad (34)$$

It is shown in [19] that the velocity \mathbf{u}_h^r , solution of the reduced problem (34), coincides exactly with the velocity \mathbf{u}_h , solution of the discretized problem (31), while the pressure p_h^0 is just the L^2 -projection of the pressure p_h on piecewise constants. Clearly, if one is interested only in the velocity field, the problem is solved. If one is also interested in the pressure part, one can just use the equation (31) and compute p_h knowing \mathbf{u}_h .

In Figs. 15–18, concerning the degrees of freedom in each element, this reduction would amount to take out all the green dots in the velocity spaces, and all the pressure dots but one.

Considering again the simplest case $k = 2$, we can perform an analysis of the local reduced space $\mathcal{V}_2^r(\mathcal{P})$ defined in (33), whose dimension, on triangular polygons, is just 12. This is equal to the number of \mathbb{P}_2 pairs in two dimensions, but the VEM space does not coincide with it. Indeed, the divergence of vectors in $(\mathbb{P}_2)^2$ is (in general) in \mathbb{P}_1 while the divergences of $\mathcal{V}_2^r(\mathcal{P})$ are all constants. Hence the property

$$(\mathbb{P}_2)^2 \subseteq \mathcal{V}_k^r(\mathcal{P})$$

is clearly lost, although we still contain all pairs of polynomials in $(\mathbb{P}_1)^2$, and all polynomials of \mathbb{P}_2 with constant divergence. Hence the *patch test* still holds in the form *if the solution \mathbf{u} is a polynomial of degree k with constant divergence, then $\mathbf{u}_h = \mathbf{u}$* . Note that this includes the incompressible case.

Note as well that (still on triangles) $(\mathbb{P}_2)^2$ and $\mathcal{V}_2^r(\mathcal{P})$ have the same dimension, but in $\mathcal{V}_2^r(\mathcal{P})$ there are two independent elements not belonging to $(\mathbb{P}_2)^2$ (the two functions in (32)). Viceversa, in $(\mathbb{P}_2)^2$ there are two elements that do not belong to $\mathcal{V}_2^r(\mathcal{P})$, as for instance,

$$\mathbf{q}^1 := \frac{1}{2}((x_1 - b_1)^2, 0) \quad \text{and} \quad \mathbf{q}^2 := \frac{1}{2}(0, (x_2 - b_2)^2),$$

where again (b_1, b_2) are the coordinates of the barycenter of \mathcal{P} .

Remark 9 Once the reduced problem has been solved (and $\mathbf{u}_h^r \equiv \mathbf{u}_h$ has been computed), the full value of the pressure p_h can be computed, in each element \mathcal{P} , using its local mean value (equal to p_h^0) and recovering the linear part (with zero mean value) by taking, in (31), \mathbf{v}_h equal to β_1 and β_2 , defined in (32).

The VEM approach followed so far for the Stokes problem in the two-dimensional case has been extended to the three-dimensional case in [13, 14, 19], including a study of the Stokes Complex and the extension to the Navier–Stokes problem.

Remark 10 It is interesting to point out that, at least for the lowest order case $k = 2$, the reduced elements in [19], reported here, have the same degrees of freedom of the formulation in [39] (see also [28]). A *step-by-step comparison* between the VEM approach presented here and that in [39] is however more difficult here than it was in previous situations. Actually, the only subspace in common between the two approaches, for the velocities, is $(\mathbb{P}_1)^2$. Hence, in order to shift from one method to the other we must exchange two subspaces of dimension six, that in general have no nontrivial elements in common. In particular, the VEM spaces are all made (inside each element) of smooth functions, whereas the others are piecewise polynomials on the refined grid but, in general, only C^0 within each element of the coarser grid.

6 Hellinger–Reissner Formulation of Linear Elasticity Problems

6.1 The Problem and its Difficulties

Starting, for simplicity, from the 2-dimensional case with homogeneous Dirichlet boundary conditions, we recall that the mixed (Hellinger–Reissner) formulation of linear elasticity problems in a domain Ω can be formulated as: Find $(\boldsymbol{\sigma}, \mathbf{u})$ in $\boldsymbol{\Sigma} \times \mathbf{U}$ such that

$$\begin{aligned} \mathbf{div} \boldsymbol{\sigma} + \mathbf{f} &= 0 & \text{in } \Omega, \\ \boldsymbol{\sigma} &= \mathbb{C}(\boldsymbol{\varepsilon}(\mathbf{u})) & \text{in } \Omega, \\ \mathbf{u} &= \mathbf{0} & \text{on } \partial\Omega, \end{aligned} \quad (35)$$

where the stress space $\boldsymbol{\Sigma} \equiv \mathbf{H}(\mathbf{div}; \Omega; \mathbb{S})$ is the space of 2×2 symmetric tensors with divergence in $(L^2(\Omega))^2$, the displacement space \mathbf{U} is $(H_0^1(\Omega))^2$, and the constitutive law is (still for simplicity) the classical $\mathbb{C}\boldsymbol{\varepsilon} := 2\mu\boldsymbol{\varepsilon} + \lambda\text{tr}(\boldsymbol{\varepsilon})$. With a common notation we also set $\mathbb{D} := \mathbb{C}^{-1}$. Defining the bilinear forms (*local* and *global*)

$$a^{\mathcal{P}}(\boldsymbol{\sigma}, \boldsymbol{\tau}) := \int_{\mathcal{P}} \mathbb{D}\boldsymbol{\sigma} : \boldsymbol{\tau} \, dx \quad \forall \mathcal{P} \quad \text{and} \quad a(\boldsymbol{\sigma}, \boldsymbol{\tau}) := \sum_{\mathcal{P}} a^{\mathcal{P}}(\boldsymbol{\sigma}, \boldsymbol{\tau}), \quad (36)$$

$$b^{\mathcal{P}}(\boldsymbol{\tau}, \mathbf{v}) := \int_{\mathcal{P}} \mathbf{div} \boldsymbol{\tau} \cdot \mathbf{v} \, dx \quad \forall \mathcal{P} \quad \text{and} \quad b(\boldsymbol{\tau}, \mathbf{v}) := \sum_{\mathcal{P}} b^{\mathcal{P}}(\boldsymbol{\tau}, \mathbf{v}), \quad (37)$$

the variational formulation of (35) can be written as: find $\boldsymbol{\sigma} \in \boldsymbol{\Sigma}$ and $\mathbf{u} \in \mathbf{U}$ such that

$$\begin{cases} a(\boldsymbol{\sigma}, \boldsymbol{\tau}) + b(\boldsymbol{\tau}, \mathbf{u}) = 0 & \forall \boldsymbol{\tau} \in \boldsymbol{\Sigma}, \\ b(\boldsymbol{\sigma}, \mathbf{v}) = -(\mathbf{f}, \mathbf{v}) & \forall \mathbf{v} \in \mathbf{U}. \end{cases}$$

Choosing suitable finite dimensional subspaces $\boldsymbol{\Sigma}_h \subset \boldsymbol{\Sigma}$ and $\mathbf{U}_h \subset \mathbf{U}$ and possibly some approximate bilinear forms a_h, b_h , and forcing term \mathbf{f}_h , the approximate problem would look like: find $\boldsymbol{\sigma}_h \in \boldsymbol{\Sigma}_h$ and $\mathbf{u}_h \in \mathbf{U}_h$ such that

$$\begin{cases} a_h(\boldsymbol{\sigma}_h, \boldsymbol{\tau}_h) + b_h(\boldsymbol{\tau}_h, \mathbf{u}_h) = 0 & \forall \boldsymbol{\tau}_h \in \boldsymbol{\Sigma}_h, \\ b_h(\boldsymbol{\sigma}_h, \mathbf{v}_h) = -(\mathbf{f}_h, \mathbf{v}_h) & \forall \mathbf{v}_h \in \mathbf{U}_h. \end{cases} \quad (38)$$

The difficulties in the Finite Element discretization of this problem come from the combined targets of

- i) getting a *symmetric* discrete stress tensor,
- ii) getting a discrete stress tensor with *continuous tractions* at interelement boundaries,
- iii) getting a *stable pair* $(\boldsymbol{\Sigma}_h, \mathbf{U}_h)$ (meaning that the *inf-sup* condition holds), and
- iv) making the formulation *hybridizable*, introducing interelement multipliers to force the continuity of tractions, and eliminating the stress field by static condensation (de Veubeke style. See also [7]).

Furthermore, it would also be nice to have (at least when the material properties are piecewise constant)

- v) the *self-equilibrium* property (meaning that if $\mathbf{f} = 0$ in one element, then $\mathbf{div} \boldsymbol{\sigma}_h = 0$ there), and
- vi) the *patch-test* of some order $k \geq 1$ (that is: if \mathbf{u} is, globally, a polynomial of degree $\leq k$, then $\mathbf{u}_h = \mathbf{u}$ and $\boldsymbol{\sigma}_h = \boldsymbol{\sigma}$).

To our knowledge, in the Finite Element framework all the above properties are almost impossible to satisfy at the same time (and we are not aware of a successful attempt) sticking on *polynomial spaces in each element*. See e.g. [5, 8, 9, 25, 27, 35, 36, 38, 42–46], and the references therein, for several important results in this direction. In a sense, the huge amount of papers that appeared in the last ten years on the subject shows, at the same time, the relevance and the difficulty of the task. On the other hand, in the VEM framework, allowing a much wider set of functions in the discrete space, *everything is possible* (...well..., “almost”). However, even the super-powerful VEM framework starts becoming complicated, and here, following essentially [11], we will limit our description to the 2-d case, referring to [31] for the (successful!) treatment of the three-dimensional case.

6.2 The VEM Spaces

Given a polygon \mathcal{P} with n edges, we first introduce the space of local infinitesimal rigid body motions:

$$RM(\mathcal{P}) = \{\mathbf{r}(\mathbf{x}) = \mathbf{a} + b(\mathbf{x} - \mathbf{x}_{\mathcal{P}})^\perp \text{ with } \mathbf{a} \in \mathbb{R}^2 \text{ and } b \in \mathbb{R}\}$$

where $\mathbf{x}_{\mathcal{P}}$ is the baricenter of \mathcal{P} . Introducing also the space

$$RM_k^\perp(\mathcal{P}) = \left\{ \mathbf{p} \in (\mathbb{P}_k)^2 : \int_{\mathcal{P}} \mathbf{p}_k \cdot \mathbf{r} = 0 \forall \mathbf{r} \in RM(\mathcal{P}) \right\},$$

we note that, obviously, we can always decompose $(\mathbb{P}_k)^2$ as a direct sum

$$(\mathbb{P}_k)^2 = RM(\mathcal{P}) \oplus RM_k^\perp.$$

For each integer $k \geq 1$ and for each polygon \mathcal{P} we now introduce the local tensor space of discretized stresses as

$$\begin{aligned} \Sigma_k(\mathcal{P}) := \{ & \boldsymbol{\tau} \in \mathbf{H}(\mathbf{div}; \Omega; \mathbb{S}) \text{ s.t. } \mathit{curlcurl}(\mathbb{D}\boldsymbol{\tau}) = 0, \\ & \boldsymbol{\tau} \cdot \mathbf{n}|_e \in (\mathbb{P}_k(e))^2 \forall e \in \partial\mathcal{P}, \mathbf{div} \boldsymbol{\tau} \in (\mathbb{P}_k)^2 \}. \end{aligned}$$

We recall that $\mathbb{D} := \mathbb{C}^{-1}$, and that the $\mathit{curlcurl}$ of a 2×2 symmetric tensor \mathbf{z} is defined as

$$\mathit{curlcurl}(\mathbf{z}) := (z_{11})_{yy} - 2(z_{12})_{xy} + (z_{22})_{xx}$$

so that for every (smooth enough) vector \mathbf{v} we have $\mathit{curlcurl}(\boldsymbol{\varepsilon}(\mathbf{v})) \equiv 0$. Hence the condition $\mathit{curlcurl}(\mathbb{D}\boldsymbol{\tau}) = 0$ is equivalent to require that $\boldsymbol{\tau} = \mathbb{C}(\boldsymbol{\varepsilon}(\mathbf{v}))$ for some vector \mathbf{v} . A natural requirement for a stress field.

A tensor $\boldsymbol{\tau} \in \Sigma_k(\mathcal{P})$ can be individuated by the following degrees of freedom:

$$\begin{aligned} \text{for each edge } e \text{ in } \partial\mathcal{P} : & \int_e \boldsymbol{\tau} \mathbf{n} \cdot \mathbf{q}_k \, ds \quad \forall \mathbf{q}_k \in (\mathbb{P}_k(e))^2, \\ \text{in } \mathcal{P} : & \int_{\mathcal{P}} \mathbf{div} \boldsymbol{\tau} \cdot \mathbf{q}_k \, dx \quad \forall \mathbf{q}_k \in (RM)_k^\perp. \end{aligned} \quad (39)$$

Remark 11 In [10] one could find a cheaper variant of the lowest order space, where $\boldsymbol{\tau} \cdot \mathbf{n}$ is required to have the normal component (i.e., τ_{nn}) linear, and the tangential component (i.e., τ_{nt}) constant, saving one degree of freedom per edge.

For the approximation of the vector space of displacements \mathbf{U} we simply take

$$\mathbf{U}_k(\mathcal{P}) := (\mathbb{P}_k)^2. \quad (40)$$

From the local spaces $\Sigma_k(\mathcal{P})$ one can then easily construct the global spaces $\Sigma(\Omega)$ by using the local spaces in each element of a decomposition, obviously making the degrees of freedom on edges *single valued*, so that the resulting space is a subspace of $\mathbf{H}(\mathbf{div}; \Omega; \mathbb{S})$. Similarly, from the local spaces (40) one constructs the global space \mathbf{U}_h for the approximation of displacements (no continuity requirements are needed here).

Using the degrees of freedom (39) we can now proceed, as we did in the previous sections, to the construction of a discrete version of the bilinear form $a^{\mathcal{P}}(\sigma, \tau)$ defined in (36). For this, we note that for every polygon \mathcal{P} , and for every τ in $\Sigma_k(\mathcal{P})$, integrating by parts we can compute the projection $\Pi_k^a \tau$ of τ onto the space $(\mathbb{P}_k)_{sym}^4$, given by

$$a^{\mathcal{P}}(\Pi_k^a \tau - \tau, \mathbf{p}_k) = 0 \quad \forall \mathbf{p}_k \in (\mathbb{P}_k)_{sym}^4.$$

We can also compute $\mathbf{div} \tau$, that belongs to $(\mathbb{P}_k)^2$. Proceeding as in all previous cases we can then define on each element \mathcal{P} an approximated bilinear form

$$a_h^{\mathcal{P}}(\sigma_h, \tau_h) := a^{\mathcal{P}}(\Pi_k^a \sigma, \Pi_k^a \tau_h) + S^{\mathcal{P}}((I - \Pi_k^a) \sigma_h, (I - \Pi_k^a) \tau_h) \quad \forall \sigma_h, \tau_h \in \Sigma_k(\mathcal{P}),$$

where again the bilinear form S is a stabilizing term (to fix ideas, of the *dofi-dofi* type). Then one gets the global bilinear form $a_h(\cdot, \cdot)$ summing over the elements. On the other hand, no projection is needed for the second equation of (38) since both the divergence of tensors in Σ_h and the elements of \mathbf{U}_h are polynomials.

We point out that VEM spaces enjoy, at the same time, all these useful features:

- A - They pass the patch test (of order k).
- B - They are easily hybridizable (having no vertex degrees of freedom).
- C - The stress field is symmetric (equilibrium of momentums).
- D - If the load $\mathbf{f} \in (\mathbb{P}_k)^2$, then $\mathbf{div} \sigma_h + \mathbf{f} = 0$ (equilibrium of forces).
- E - The definition, essentially, does not depend on the *shape* of the elements (triangles, quads, polygons, polyhedra etc.)

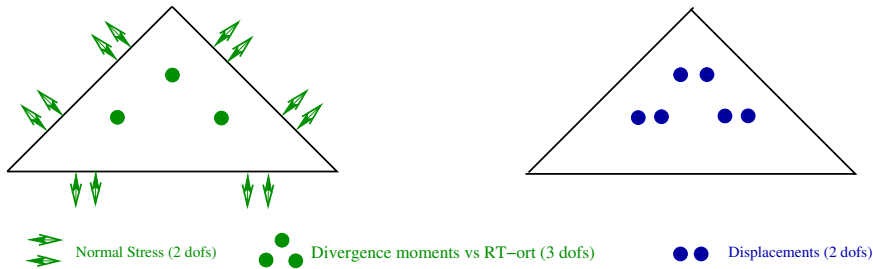


Fig. 19 Hellinger-Reissner Dofs for $k = 1$, VEM [11]

As we already did in the previous section (on Stokes problem), we will not enter a detailed comparison between VEM and different types of FEM. Among other things, this is also due to the difficulty to pick-up one or two typical Finite Element approaches for the comparison.

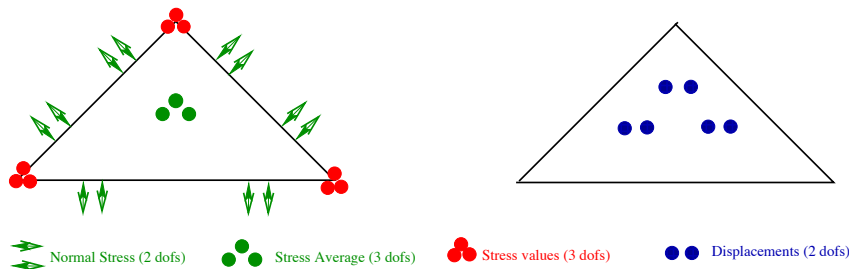


Fig. 20 Hellinger-Reissner Dofs for $k = 1$, FEM Arnold-Winther [5]

Actually, by now, we have a very wide variety of FEM to deal with the present problem. To our knowledge, the paper [38] (using *rational functions* together with polynomials) is the one that best approaches, on triangles, the basic features of VEM. One might consider that rational functions are used there, instead of *solutions of some PDE system* (as we do with VEM) as an alternative way to escape the *polynomial trap*. In our figures 19 and 20 we decided however to compare the degrees of freedom of VEM with those of the most classical (and possibly best known) [5], hence avoiding a description of the FEM spaces used in more recent approaches. We do not pretend this to be exhaustive in any sense. It is not, BY FAR. We refer the interested readers to the FEM and VEM papers already cited here.

References

1. Ahmad, B., Alsaedi, A., Brezzi, F., Marini, L.D., Russo, A.: Equivalent projectors for virtual element methods. *Comput. Math. Appl.* **66**, 376–391 (2013)
2. Antonietti, P.F., Manzini, G., Verani, M.: The fully nonconforming virtual element method for biharmonic problems. *Math. Models Methods Appl. Sci.* **28**, 387–407 (2018)
3. Arnold, D.N., Awanou, G.: The serendipity family of finite elements. *Found. Comput. Math.* **11**, 337–344 (2011)
4. Arnold, D.N., Awanou, G., Boffi, D., Bonizzoni, F., Falk, R.S., Winther, R.: The periodic table of finite elements. To appear (2015)
5. Arnold, D.N., Awanou, G., Winther, R.: Finite elements for symmetric tensors in three dimensions. *Math. Comput.* **77**, 1229–1251 (2008)
6. Arnold, D.N., Boffi, D., Falk, R.S.: Approximation by quadrilateral finite elements. *Math. Comput.* **71**, 909–922 (2002)
7. Arnold, D.N., Brezzi, F.: Mixed and nonconforming finite element methods: implementation, postprocessing and error estimates. *RAIRO Modél. Math. Anal. Numér.* **19**, 7–32 (1985)
8. Arnold, D.N., Falk, R.S., Winther, R.: Differential complexes and stability of finite element methods II. The elasticity complex. In: Arnold, D.N. et al. (eds.) *Compatible Spatial Discretizations*. The IMA Volumes in Mathematics and its Applications, vol. 142, pp. 47–67. Springer, New York (2006)
9. Arnold, D.N., Falk, R.S., Winther, R.: Mixed finite element methods for linear elasticity with weakly imposed symmetry. *Math. Comput.* **76**, 1699–1723 (2007)
10. Artioli, E., de Miranda, S., Lovadina, C., Patruno, L.: A stress/displacement virtual element method for plane elasticity problems. *Comput. Methods Appl. Mech. Eng.* **325**, 155–174 (2017)
11. Artioli, E., de Miranda, S., Lovadina, C., Patruno, L.: A family of virtual element methods for plane elasticity problems based on the Hellinger–Reissner principle. *Comput. Methods Appl. Mech. Eng.* **340**, 978–999 (2018)
12. Ayuso de Dios, B., Lipnikov, K., Manzini, G.: The nonconforming virtual element method. *ESAIM Math. Model. Numer. Anal.* **50**, 879–904 (2016)
13. Beirão da Veiga, L., Dassi, F., Vacca, G.: The Stokes complex for Virtual Elements in three dimensions. *Math. Models Methods Appl. Sci.* **30**, 477–512 (2020)
14. Beirão da Veiga, L., Mora, D., Vacca, G.: The Stokes complex for virtual elements with application to Navier–Stokes flows. *J. Sci. Comput.* **81**, 990–1018 (2019)

15. Beirão da Veiga, L., Brezzi, F., Cangiani, A., Manzini, G., Marini, L.D., Russo, A.: Basic principles of virtual element methods. *Math. Models Methods Appl. Sci.* **23**, 199–214 (2013)
16. Beirão da Veiga, L., Brezzi, F., Marini, L.D., Russo, A.: $H(\text{div})$ and $H(\text{curl})$ -conforming VEM. *Numer. Math.* **133**, 303–332 (2016)
17. Beirão da Veiga, L., Brezzi, F., Marini, L.D., Russo, A.: Serendipity nodal VEM spaces. *Comput. Fluids* **141**, 2–12 (2016)
18. Beirão da Veiga, L., Brezzi, F., Marini, L.D., Russo, A.: Serendipity face and edge VEM spaces. *Rend. Lincei Mat. Appl.* **28**, 143–180 (2017)
19. Beirão da Veiga, L., Lovadina, C., Vacca, G.: Virtual elements for the Navier–Stokes problem on polygonal meshes. *SIAM J. Numer. Anal.* **56**, 1210–1242 (2018)
20. Boffi, D., Brezzi, F., Fortin, M.: *Mixed Finite Element Methods and Applications*. Springer Series in Computational Mathematics, vol. 44. Springer, Berlin, Heidelberg (2013)
21. Brezzi, F., Jr Douglas, J., Marini, L.D.: Two families of mixed finite elements for second order elliptic problems. *Numer. Math.* **47**, 217–235 (1985)
22. Brezzi, F., Falk, R.S., Marini, L.D.: Basic principles of mixed virtual element methods. *ESAIM Math. Model. Numer. Anal.* **48**, 1227–1240 (2014)
23. Brezzi, F., Fortin, M.: *Mixed and Hybrid Finite Element Methods*. Springer Series in Computational Mathematics, vol. 15. Springer, New York (1991)
24. Brezzi, F., Marini, L.D.: Virtual element methods for plate bending problems. *Comput. Methods Appl. Mech. Eng.* **253**, 455–462 (2013)
25. Chen, L., Hu, J., Huang, X.: Stabilized mixed finite element methods for linear elasticity on simplicial grids in \mathbb{R}^n . *Comput. Methods Appl. Math.* **17**, 17–31 (2017)
26. Chinosi, C., Marini, L.D.: Virtual element method for fourth order problems: L^2 -estimates. *Comput. Math. Appl.* **72**, 1959–1967 (2016)
27. Christiansen, S.H., Hu, J., Hu, K.: Nodal finite element de Rham complexes. *Numer. Math.* **139**, 411–446 (2018)
28. Christiansen, S.H., Hu, K.: Generalized finite element systems for smooth differential forms and Stokes’ problem. *Numer. Math.* **140**, 327–371 (2018)
29. Ciarlet, P.G.: *The Finite Element Method for Elliptic Problems*. Studies in Mathematics and its Applications, vol. 4. North-Holland Publishing Co., Amsterdam, New York, Oxford (1978)
30. Crouzeix, M., Raviart, P.-A.: Conforming and nonconforming finite element methods for solving the stationary Stokes equations I. *Rev. Fr. Autom. Inform. Rech. Opér. Sér. Rouge* **7**, 33–75 (1973)
31. Dassi, F., Lovadina, C., Visinoni, M.: A three-dimensional Hellinger–Reissner Virtual Element Method for linear elasticity problems. *Comput. Methods Appl. Mech. Eng.* **364**, 112910 (2020)
32. Falk, R.S., Neilan, M.: Stokes complexes and the construction of stable finite elements with pointwise mass conservation. *SIAM J. Numer. Anal.* **51**, 1308–1326 (2013)
33. Fortin, M., Soulie, M.: A non-conforming piecewise quadratic finite element on triangles. *Int. J. Numer. Methods Eng.* **19**, 505–520 (1983)
34. Fu, G., Guzmán, J., Neilan, M.: Exact smooth piecewise polynomial sequences on Alfeld splits. *Math. Comput.* **89**, 1059–1091 (2020)
35. Gong, S., Wu, S., Xu, J.: New hybridized mixed methods for linear elasticity and optimal multilevel solvers. *Numer. Math.* **141**, 569–604 (2019)
36. Gopalakrishnan, J., Guzmán, J.: A second elasticity element using the matrix bubble. *IMA J. Numer. Anal.* **32**, 352–372 (2012)
37. Guzmán, J., Neilan, M.: Conforming and divergence-free Stokes elements on general triangular meshes. *Math. Comput.* **83**, 15–36 (2014)
38. Guzmán, J., Neilan, M.: Symmetric and conforming mixed finite elements for plane elasticity using rational bubble functions. *Numer. Math.* **126**, 153–171 (2014)
39. Guzmán, J., Neilan, M.: Inf-sup stable finite elements on barycentric refinements producing divergence-free approximations in arbitrary dimensions. *SIAM J. Numer. Anal.* **56**, 2826–2844 (2018)
40. Guzmán, J., Scott, L.R.: Cubic Lagrange elements satisfying exact incompressibility. *SMAI J. Comput. Math.* **4**, 345–374 (2018)
41. Guzmán, J., Scott, L.R.: The Scott–Vogelius finite elements revisited. *Math. Comput.* **88**, 515–529 (2019)
42. Hu, J.: Finite element approximations of symmetric tensors on simplicial grids in \mathbb{R}^n : the higher order case. *J. Comput. Math.* **33**, 283–296 (2015)
43. Hu, J.: A new family of efficient conforming mixed finite elements on both rectangular and cuboid meshes for linear elasticity in the symmetric formulation. *SIAM J. Numer. Anal.* **53**, 1438–1463 (2015)
44. Hu, J., Ma, R.: Conforming mixed triangular prism elements for the linear elasticity problem. *Int. J. Numer. Anal. Model.* **15**, 228–242 (2018)
45. Hu, J., Zhang, S.: A family of symmetric mixed finite elements for linear elasticity on tetrahedral grids. *Sci. China Math.* **58**, 297–307 (2015)

46. Hu, J., Zhang, S.: Finite element approximations of symmetric tensors on simplicial grids in \mathbb{R}^n : the lower order case. *Math. Models Methods Appl. Sci.* **26**, 1649–1669 (2016)
47. John, V., Linke, A., Merdon, Ch., Neilan, M., Rebholz, L.G.: On the divergence constraint in mixed finite element methods for incompressible flows. *SIAM Rev.* **59**, 492–544 (2017)
48. Mascotto, L., Pichler, A.: Extension of the nonconforming Trefftz virtual element method to the Helmholtz problem with piecewise constant wave number. *Appl. Numer. Math.* **155**, 160–180 (2020)
49. Nédélec, J.-C.: Mixed finite elements in \mathbb{R}^3 . *Numer. Math.* **35**, 315–341 (1980)
50. Nédélec, J.-C.: A new family of mixed finite elements in \mathbb{R}^3 . *Numer. Math.* **50**, 57–81 (1986)
51. Raviart, P.-A., Thomas, J.M.: A mixed finite element method for 2nd order elliptic problems. In: Galligani, I., Magenes, E. (eds.) *Mathematical Aspects of Finite Element Methods (Proceedings of the Conference Held in Rome, December 10–12, 1975)*. Lecture Notes in Mathematics, vol. 606, pp. 292–315. Springer, Berlin, Heidelberg (1977)
52. Zhang, S.: A family of $Q_{k+1,k} \times Q_{k,k+1}$ divergence-free finite elements on rectangular grids. *SIAM J. Numer. Anal.* **47**, 2090–2107 (2009)
53. Zhao, J., Chen, S., Zhang, B.: The nonconforming virtual element method for plate bending problems. *Math. Models Methods Appl. Sci.* **26**, 1671–1687 (2016)
54. Zienkiewicz, O.C., Taylor, R.L., Zhu, J.Z.: *The Finite Element Method: Its Basis and Fundamentals*, 7th edn. Elsevier/Butterworth Heinemann, Amsterdam (2013)